Annales Societatis Geologorum Poloniae (1994), vol. 63: 211 - 248
PL ISSN 0208-9068

ORGANODETRITAL CONGLOMERATES WITH OOIDS IN THE CIESZYN LIMESTONE (TITHONIAN - BERRIASIAN) OF THE POLISH FLYSCH CARPATHIANS AND THEIR PALAEOGEOGRAPHIC SIGNIFICANCE

Jacek Matyszkiewicz & Tadeusz Słomka

Faculty of Geology, Geophysics & Environmental Protection, University of Mining & Metallurgy, Al. Mickiewicza 30, 30-059 Kraków, Poland

Matyszkiewicz J. & Słomka T., 1994. Organodetrital conglomerates with ooids in the Cieszyn Limestone (Tithonian-Berriasian) of the Polish Flysch Carpathians and their palaeogeographic significance. *Ann. Soc. Geol. Polon.*, 63: 211 – 248.

Abstract: Several beds of organodetrital conglomerates containing ooids were found in the carbonate turbidites of the Upper Cieszyn Limestone (Berriasian) of the Żywiec region. Three microfacies were distinguished: oolithic-sponge, sponge and pyritic-algal. Their presence prooves fluorishing life on the shallow-water carbonate platform of the Silesian Ridge at the transition of Jurassic to Cretaceous time, and points to the progressive eastward migration of tectonic movements responsible for the uplift of successive tectonic blocks within the Ridge. Denudation of the uplifted areas supplied large volumes of calcareous debris which was deposited along the foot of the Silesian Ridge, first as aprons, then as submarine fans.

Key words: Cieszyn Limestone, microfacies, ooids, Berriasian, palaeogeography, Outer Carpathians

Manuscript received 21 October 1993, accepted 30 July 1994

INTRODUCTION

The Silesian Ridge was an important palaeogeographic element of the Carpathian Geosyncline, separating the Magura and Silesian sedimentary basins. Its existence as a vast, uplifted terrain at the end of the Jurassic time is widely accepted (Książkiewicz, 1951, 1956, 1960; Eliáš & Eliášová, 1984). However, the source area of clastic material during sedimentation of the Cieszyn Limestone (Tithonian - Berriasian) is still a matter of discussion. Two concepts have been proposed. According to Książkiewicz (1956, 1960), Peszat (1967) and Malik (1986) the source areas were exclusively the north-western and northern continental margins of the Silesian Basin currently identified as the Inwałd Ridge (= Baška-Inwałd Ridge). Other authors (Nowak, 1973; Słomka,

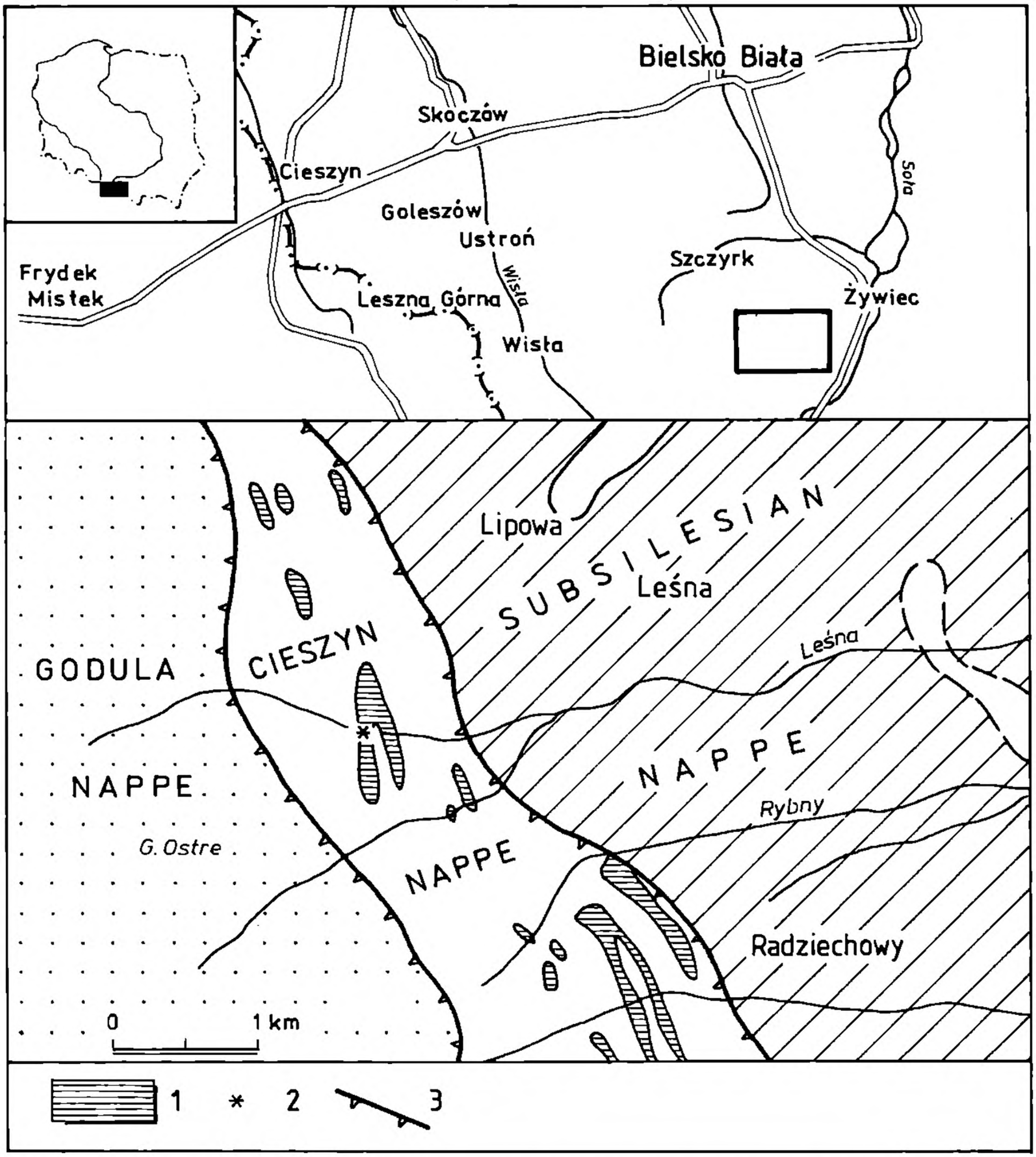

Fig. 1 Location of studied area (after Nowak, 1966; Żytko, 1966, simplified): *1* – Cieszyn Limestones; *2* – outcrops with organodetrital conglomerate layer; *3* – thrust

Lokalizacja rejonu badań na tle mapy topograficznej i geologicznej (wg. Nowak, 1966; Żytko, 1966; uproszczone): *1* – wapienie cieszyńskie; *2* – usytuowanie wychodni z ławicami zlepieńców organodetrytycznych z ooidami; *3* – nasunięcie

1986a; Krobicki, 1993) suggested an additional contribution from islands located at the western margins of the Silesian Ridge.

The Cieszyn Limestone cropping out in the valley of Leśna Stream near Żywiec (Fig. 1) comprises several layers of distinctive conglomerates. They include limestone pebbles as well as numerous ooids, other coated grains and relics of fossils. The results of microfacies analysis of samples from this locality contribute to the palaeoecological and palaeogeographical reconstructions of both the Silesian Ridge and the Silesian Basin.

This research has been supported financially by the Faculty of Geology, Geophysics & Environmental Protection, University of Mining & Metallurgy in Kraków.

GEOLOGICAL SETTING

The Cieszyn Beds (Kimmeridgian-Hauterivian) are the oldest stratigraphical division of the Silesian Nappe in the Outer Carpathians and are traditionally subdivided into three subunits: the Lower Cieszyn Shales, the Cieszyn Limestone and the Upper Cieszyn Shales (Hohenegger, 1861) (Fig. 2). Structurally, the Cieszyn Beds belong to the lower part of the Silesian Nappe – the so-called Cieszyn Nappe (Nowak, 1927) which is known from the mountain ranges of the Moravian-Silesian, Beskid Silesian and Small Beskid.

The Cieszyn Limestone (Tithonian-Berriasian) of highly variable thickness (maximum 250 metres) consists of calcareous flysch (Książkiewicz, 1960, Peszat, 1967). The sequence is dominated by detrital, organodetrital and pelitic limestones intercalated by marly shales. Limestone breccias and conglomerates as well as calcareous sandstones are less common. Comprehensive data on the stratigraphy, lithology and origin of the Cieszyn Limestones are provided by Peszat (1967), Eliáš (1970), Książkiewicz (1971), Nowak (1973), Mišik (1974), Malik (1986) and Słomka (1986a).

In the Żywiec Depression, the Cieszyn Limestone crops out in an anticlinal structure of the Grójec Mały massif and in some slice-folds which extend in a belt Przybędza-Radziechowy-Lipowa (Fig. 1). Maximum thickness of the unit attains 180 metres. The limestones in Żywiec area is similar in lithology to those from Goleszów (Peszat, 1967; Malik, 1986, Slomka, 1986a). Two subunits are distinguished (Fig. 2A): the Lower Cieszyn Limestone which comprises detrital, pelitic and mixed limestones intercalated by marly shales and the Upper Cieszyn Limestone which includes detrital and organodetrital limestones interbedded by marly shales. Interbeds of arenaceous detrital limestones appear upwards in the sequence in places with calcareous sandstones. In the section along the Soła river the latter are the dominant rock type in the upper part of the unit (Tokarski, 1947).

The Cieszyn Limestone cropping out in the Leśna Stream valley (Fig. 1) includes fragments of both the lower and upper subunit. The rocks are strongly folded, sheared and extremely densly fractured. Several conglomerate layers were found in the Upper Cieszyn Limestones. These conglomerates vary in thickness from 30 to 100 cm. The main components are pebbles of micritic limestones with minor ooids, other coated grains and relics of calcareous algae, hydrozoans, molluscs, brachiopods, bryozoans and echino-

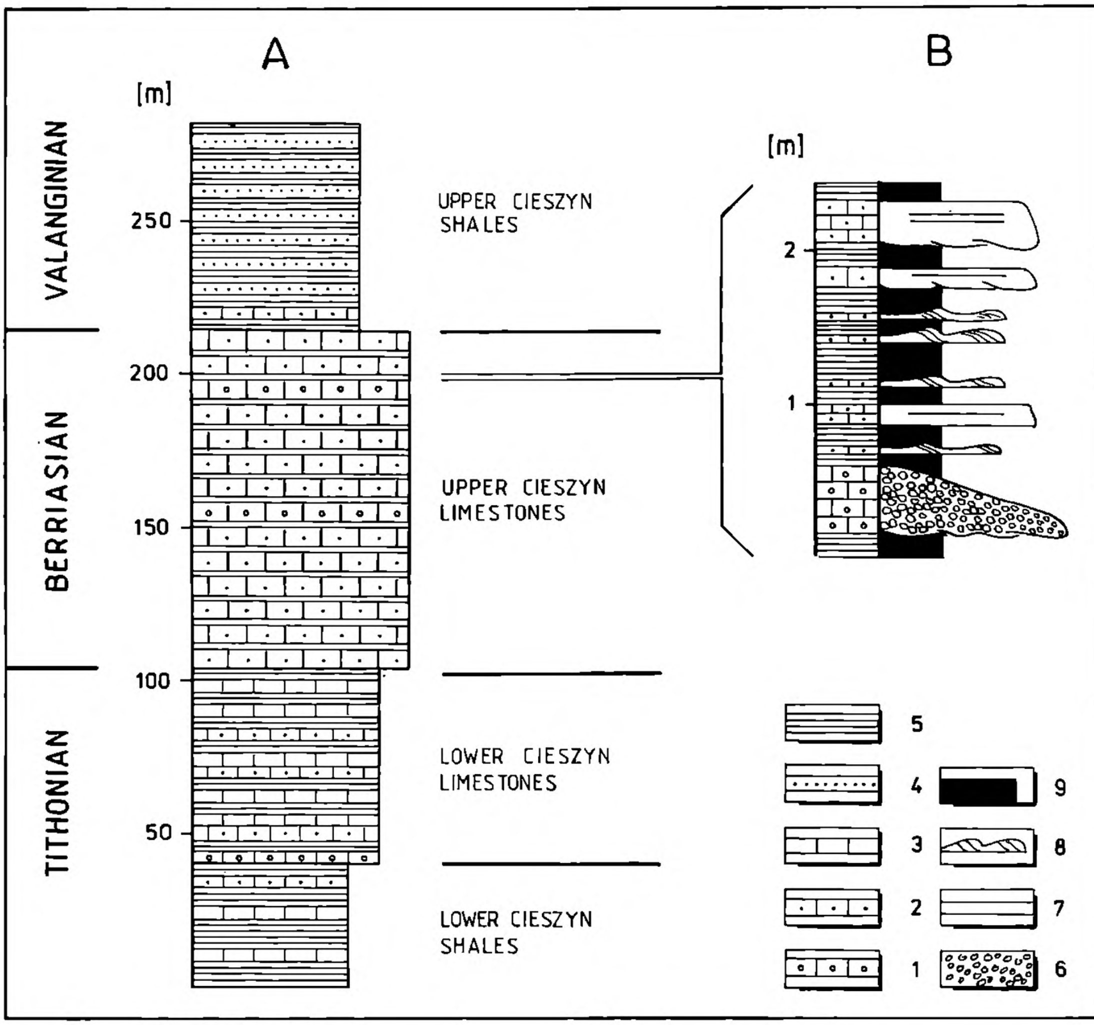

Fig. 2 A. Schematic lithostratigraphic profile of the Cieszyn Beds in Żywiec area. B. Fragment of profile with the layer of organodetrital limestones with ooids: *1* – limestone conglomerates; *2* – detrital limestones; *3* – pelitic limestones; *4* – calcareous sandstones; *5* – marly shales; sedimentary structures: *6* – massive; *7* – parallel lamination; *8* – ripplemark cross-lamination, *9* – structureless shale

A. Schematyczny profil litostratygraficzny warstw cieszyńskich w rejonie Żywca. B. Fragment profilu z ławicą zlepieńca organo-detrytycznego z ooidami: *1* – zlepieńce wapienne; *2* – wapienie detrytyczne; *3* – wapienie pelityczne; *4* – piaskowce wapniste; *5* – łupki margliste; struktury sedymentacyjne: *6* – masywna; *7* – laminacja równoległa; *8* – laminacja przekątna riplemarkowa; *9* – bezstrukturowy łupek

derms. One of the studied layers contains a high percentage of ooids, calcareous algae and sponges.

A precise stratigraphic position of this layer in the sequence is unknown owing to the strong tectonism which mixed together fragments of limestone and shale beds. The undisturbed part of the sequence is about 2 metres thick (Fig. 1B) and consists of thin and very thin layers of dark and ash-grey detrital limestones with parallel and cross-lamination, intercalated by thin, greyish-green, marly shales. The conglomerate layer is up to 48 cm thick. These conglomerate lenses, each of different strike and thickness, occur within a lateral distance of several metres. These probably represent tectonic fragmentation of an initially continuous layer. The longest observed lens was 2.5 m long and 26 cm thick, but the largest fragment is now covered by a small stone dam. The bottom surface of the layer shows flat, shallow loadcasts whereas the top surface is wavey. The grain components are limestone and dolomite pebbles, fragments of calcareous algae, ooids and other coated grains. Other organic relics are bivalves, ammonites, gastropods, brachiopods, echinoderms, corals and foraminifers. The grain diameters reach 3 cm and the percentage of grain components varies from 30 to 70%. All components are randomly distributed, both vertically and laterally. A characteristic feature is the presence of local enrichments of some components in the form of nests and streaks.

COMPONENTS OF MICROFACIES

Microfacies were studied mostly in one layer with supplementary data from the other layers. The following microfacies have been distinguished:

— oolithic-sponge,
— sponge,
— pyritic-algal.

These microfacies are only an incomplete record of facies developed on the carbonate platform bordering the Silesian Ridge. Components of these microfacies are characterized below.

Ooids

Five types of ooids have been observed:

— combined radial-concentric, ellipsoidal, multilaminated, with nuclei silicified with authigenic quartz (Type 1; cf. Tucker, 1984; Strasser, 1986; Strohmenger *et al.*, 1987),

— combined radial-concentric, spheroidal, with few laminae and cortices randomly silicified with authigenic quartz (Type 2, cf. Strasser 1986; Strohmenger *et al.*, 1987),

— combined radial-concentric, spheroidal or ellipsoidal, with few laminae, and lacking silicification (Type 3; cf. Tucker, 1984; Strasser, 1986; Strohmenger *et al.*, 1987),

— radial, concentric, mono-laminae (Type 4, cf. Strasser, 1986),

— radial, eccentric, ellipsoidal, mono- or bilaminae (Type 5, cf. Carozzi, 1957; Gąsiewicz, 1984).

Type 1 ooids (Pl. I: 1-4; II: 1; III: 4) consist of numerous (up to 15), easily visible sparite or microsparite laminae concentrically growing on the nucleus and separated by micritic envelopes. Ooids are ellipsoidal with diameters, varying from 0.3 to 1.2 mm. The ratio of nucleus diameter to cortex thickness (N/C) varies from 1:0.2 to 1:4. Large, elongated nuclei (up to 1 mm across) show distinct microspar laminae over flat surfaces but not over curved edges (Pl. I: 2) such that grains increase in sphericity during growth. According to Richter (1983), this is the best diagnostic criterion which allows to distinguish between ooids and other types of grains. The length of radially arranged crystals in the laminae varies from 5 to 25 μm and it controls the thickness of the layers. Some microspar laminae show local irregularities in the radial growth of crystals. Boundaries of laminae are usually sharp. Occasionally, microsparite and sparite laminae show micritization. The nuclei usually consist of fine (over 0.5 mm) shell debris, partly replaced by authigenic quartz with calcite inclusions (Pl. I: 1, 3, 4). Sporadically, the nuclei contain large, elongated, pelmicrite intraclasts with scattered authigenic quartz crystals (Pl. I: 2). In such grains the number of microsparite or sparite envelopes is limited (3 - 4). The cortex is not affected by silicification with authigenic quartz. Some Type 1 ooids show numerous, radial cracks filled with blocky calcite cement (Pl. I: 1).

Type 1 ooids were found in the oolithic-sponge microfacies. The grains are embedded within blocky calcite cement. Locally, isopachous cement rims (up to 0.02 mm) are preserved on the grain surfaces. Sporadically these ooids also occur in pyritic matrix.

Type 2 ooids (Pl. II: 4; III: 2) are concentric forms composed of several (4 - 8) laminae, each consisting of radially arranged sparite or microsparite crystals and separated with micritic envelopes. The grain shapes are very regular and spheroidal. The diameters vary from 0.3 to 0.8 mm. N/C ratio varies from 1:2 to 1:7. Boundaries of sparite and microsparite laminae are diffuse owing to advanced micritization. Numerous authigenic quartz crystals with calcite inclusions were observed within the cortex. Spotty silicification is manifested by the presence of authigenic quartz crystals which occasionally affects also the nucleus and cracks (Pl. III: 2). The nucleus is a peloid or a micritic intraclast. The boundary between nucleus and cortex is gradual. Outer laminae do not show traces of dissolution.

Type 2 ooids were observed in the oolithic-algal facies. They are embedded in the blocky calcite cement or in the micritic matrix of intraclasts. In the former case isopachous cement rims (0.03 mm thick) can locally be preserved.

Type 3 ooids (Pl. II: 1-3; III: 1; IV: 1, 2) show poorly developed cortex composed of 1-4 radial-concentric laminae which grow on a bioclast or, rarely, on a micritic intraclast. N/C ratio exceeds 5:1 (7:1, on average). Grain diameters are very variable and may reach 1.1 mm. Nuclei contain algal fragments (*Cayeuxia* sp., *Solenopora* sp.) gastropod shells, echinoid spines and echinoderm plates. The shapes and sizes of ooids are controlled by bioclasts of the nuclei. If the bioclast was an aragonitic gastropod shell it was dissolved and replaced by micrite. Such ghosts of original particles can be observed within blocky calcite cement (Pl. II: 5). Some type 3 ooids, especially those which cortices, consist of only one lamina, are occasionaly strongly micritized, and differ not significantly from so-called simple oncoids.

Type 3 ooids occur in both the oolithic-sponge and sponge microfacies, in a matrix composed of blocky calcite cement or pyrite. Grains embedded in blocky calcite cement may show relics of isopachous cement rims or traces of dissolution of outer laminae. Dissolved parts of laminae are replaced with blocky calcite cement and single authigenic quartz crystals (Pl. II: 3). Where pyrite is the matrix, the grain boundaries locally show the presence of needle-shaped crystals (probably aragonite) up to 0.02 mm long. Such ooids are strongly micritized (Pl. III: 1; IV: 2) and cracks may be filled with authigenic quartz crystals. If the carbonate matrix is not entirely pyritized meniscus cement can be observed along the grain contacts (Richter, 1978).

Type 4 ooids (Pl. II: 3) differ markedly from the others by the presence of only one cortical lamina. The lamina consists of radially arranged sparite crystals whose lengths greatly exceed the nucleus diameter (N/C ratio 1:4). Such grains may reach up to 0.6 mm across but smaller diameters (up to about 0.3 mm) predominate. The type 4 ooids are very regular and spheroidal in shape. The nuclei are poorly visible and grade into the cortical lamina. Occasionaly, single lamina contain relics of concentric envelopes.

The type 4 ooids occur in the oolithic-sponge microfacies and are embedded within the blocky calcite cement. Isopacheous cement rims (up to 0.02 mm thick) were noticed.

Type 5 ooids are rare (Pl. IV: 1; VIII: 4) and they belong to the so called "eccentric" grains (Carozzi, 1957; Gąsiewicz, 1984). The grains are 0.5-0.7 mm across, ellipsoidal, with embankments on the surface. There are up to six sparite laminae. Nuclei consist of pelmicrite or fine shell detritus. Basic difference in comparison with the other ooid types lies in irregular (eccentric) arrangement of laminae as well as the presence of compression pits. These ooids usually deform other grains (Pl. IV: 1).

Type 5 ooids were found in both the oolithic-sponge and pyritic-algal microfacies.

Oncoids

Oncoids with well-developed internal structure occur sporadically in the Cieszyn Limestone (Pl. II: 3; IV: 4; VII: 2). They are up to 1.5 mm across, elongated or irregular. Their nuclei are always benthonic foraminifers (*Nodophthalmidium* sp.). Cortices include numerous micrite laminae of cyanobacterial origin locally separated by microspar and affected by spotty silicification with authigenic quartz. The grain boundaries show local dissolution, sometimes advanced. Such oncoids, known from the Jurassic sediments of the carbonate platform, bear the name *Tubiphytes* (see Morycowa & Moryc, 1976; Pomoni-Papaioannou *et al.*, 1989, Matyszkiewicz, 1989; Matyszkiewicz &

Felisiak, 1992). However, this form cannot be identified with *Tubiphytes* sp. described by Maslov (1956) from Palaeozoic deposits. It also differs significantly from the Tethyan *Tubiphytes* sp. (B. Senowbari-Daryan, 1992, personal communication).

Locally, so called "simple" oncoids are present (Pl. II: 5). They are between 0.2 and 0.4 mm in diameters and consist of single, micritic or locally microsparite lamina growing over fine bioclasts. Their formation by micritization of type 3 ooids can not be ruled out.

Both the *Tubiphytes* sp. and the simple oncoids were found in oolithic-sponge and sponge microfacies.

Algae

Calcareous algae are common constituents of the studied sediments. They were found to predominate in the pyritic-algal microfacies but can also be observed in other microfacies.

The most widespread in the pyritic-algal microfacies are red algae (Rhodophyceae) of the families Solenoporaceae (cf. *Solenopora* sp.; Pl. V: 1, 2) and Corallinaceae (*Marinella lugeoni* Pfender; Pl. III: 4; V: 4, 5; VIII: 4). Algae of Porostromata type (Pl. V: 3) are also abundant. These were conventionally classified as green algae (Chlorophyceae) of the family Codiaceae (*Cayeuxia* sp.) but, more recently, were ascribed to blue algae (Cyanophyceae; cf. *Rivularia* sp.) (Dragastan, 1985). The other microfacies contain representatives of the above mentioned families and, additionally, also Rhodophyceae of the family Gymnocodiaceae (cf. *Permocalculus* sp.; Pl. VI: 6).

Pyrite

Pyritization is a common process in the studied sediments. Three textures can be distinguished:

— replacement of bivalve molds (Pl. VIII: 4, 5),

— replacement of matrix (Pl. III: 1; IV: 2),

— detrital, pyritized fossil relics which are one of the two principal components of pyritic-algal facies (Pl. X: 2).

Pyritization preferentially affected molds of ammonites (mostly juvenile forms, Pl. VIII: 5) and bivalves. Replacement of aragonitic shells by pyrite led to almost complete obliteration of their internal structure. Internal spaces of chambers in ammonite shells were completely pyritized and only the most pronounced details (suture lines) have been preserved. The outlines of outer edges also remained unaffected. Cracks cutting the pyritized mollusc shells were filled with blocky calcite cement. Such pyritized shells were observed exclusively in pyritic-algal microfacies.

Pyritization of matrix enclosing the ooids is limited to single intraclasts of a diameters over 2 mm, which are abundant in the sponge microfacies. Pyrite aggregates which fill intersticial spaces consist of fine sphaeroids (about 0.01 mm across) or ellipsoids (so called ovoid textures, cf. Fisher, 1986) of similar size. Locally, rod-like crystals can be observed at the boundaries of the matrix-enclosed ooids. These are presumably relics of aragonitic cement which may occasionaly show features of meniscus cement (Richter, 1976).

Detrital pyrite which predominates in the pyritic-algal facies occurs as elongate, sharp-edged fragments up to 4 mm long and 1 mm wide. The fragments are pyritized plant detritus among which coniferous wood have been identified (M. Krąpiec, 1993, personal communication). No patterns in their distribution have been observed. Locally, detrital pyrite fragments are cracked and the cracks are filled with blocky calcite cement.

Dolomite and post-dolomite calcite

Both the dolomite and post-dolomite calcite were noticed in clasts with diameters over 1 millimeter. Dolomitizatiom is observed in dolomite clasts, partly dedolomitized (Pl. VIII: 1, 2) and in infillings of small vugs in intraclasts of typical, cyanobacterial-sponge limestones (Pl. VIII: 3).

Partly dedolomitized clasts were found in the sponge microfacies. The grains are ellipsoidal and well-rounded. Enclosing blocky calcite cement is devoid of inclusions along the clasts boundaries. The clasts are composed of idiomorphic and hipidiomorphic partly dedolomitized dolorhombs up to 0.05 mm across. Locally, framboidal pyrite aggregates (up to 0.01 mm in diameter) replace dolorhombs and fill the intersticial spaces along with brownish iron oxides and vadose silt.

Dolomite in the intraclasts of cyanobacterial-sponge limestones appears as fillings of vugs up to 1 mm in size. The vug walls are covered with thin (up to 0.15 mm) films of fibrous cement whereas the interiors are filled with hipidiomorphic dolomite crystals (up to 0.03 mm across). These crystals show partial dedolomitization and can locally be embedded in dark-brown iron oxides.

DESCRIPTIONS OF MICROFACIES

Oolithic-sponge microfacies
(Pl. I; II: 1, 3-5; III: 2-4; IV: 1; V: 1; VI: 4; VIII: 3; IX: 1)

Sediments belonging to this microfacies are classified as grainstones. Size distribution of the main clastic components is bimodal. Intraclasts of cyanobacterial-sponge limestones and detritus of thick bivalve shells are dispersed in a mass of ooids and simple oncoids of diameters less than 1 mm in size (sporadically up to 1 cm). Ooids constitute up to 25% of the rock and form occasional accumulations. Poorly rounded intraclasts of cyanobacterial-sponge limestones show local traces of dolomitization and dedolomitization, and sporadically contain eccentric ooids.

The rocks of oolithic-sponge microfacies also contain scarce foraminifers (*Ammobaculites* sp.; Pl. II: 5), hydrozoans (Pl. VI: 4) and algae. Apart from marine red algae observed as single bioclasts in blocky calcite cement, fragments of delicate *Permocalculus* sp. were noticed in the micritic matrix filling the internal parts of larger bivalve shells. Locally, large oncoids (*Tubiphytes* sp., over 1 mm in diameter) were seen. Their cortices show spotty silicification with authigenic quartz whereas grain boundaries reveal traces of dissolution.

The granular components are embedded within blocky calcite cement. Some grains have locally preserved thin (up to 0.05 mm) films of isopachous cement.

Sponge microfacies

(Pl. II: 2; III: 1; IV: 2, 3; V: 4; VI: 1-3, 5, 6; VII; VIII: 1, 2; XI: 2; X: 1)

This microfacies seems to be close to the so called "cyanobacterial-sponge facies". The main components of this microfacies are intraclasts of cyanobacterial-sponge limestones over 5 mm in size (rudstones-intrasparite). The intraclasts are irregular and poorly rounded. Some grains show well-preserved structures typical of calcified siliceous sponges (Pl. VII: 1). Apart from sponges, the fossil assemblage characteristic of this biofacies includes polychaetes (*Terebella lapilloides*, Pl. VII: 4), serpules, foraminifers (cf. *Lenticulina* sp.), *Tubiphytes* sp. which are symbiotic associations of the foraminifer *Nodophthalmidium* sp. and cyanobacteria, forms resembling spherulites (Pl. VII: 3) of inferred cyanobacterial origin (cf. Andrews, 1986; Chafetz, 1986), fine, partly dissolved gastropods shells (Pl. VI: 6), hydrozoans.

Well-rounded dolomite intraclasts occur sporadically. There are partly dedolomitized and are probably fragments of dolomitized cyanobacterial-sponge limestones.

Some intraclasts composed of ooids and pyritic matrix in the sponge microfacies presumably originate from a depositional environment different from that of the cyanobacterial-sponge limestones. It seems also that some bioclasts noticed from the sponge facies: corals (Pl. VI: 2, 3) and calcareous algae were redeposited from other environment.

The matrix of sponge microfacies is mostly the blocky calcite cement but accumulations of vadose silt are also common.

Pyritic-algal microfacies

(Pl. V: 2, 3, 5; X: 2)

Sediments of this microfacies are grainstones (intrasparite) and rudstones. Main constituents are detrital pyrite grains (25%) and algal fragments (up to

20%). Pyrite intraclasts are pyritized plant fragments among which coniferous wood has been identified. Such grains are angular and reach the length of several millimeters and width up to 1 mm. Poorly rounded pyrite intraclasts are isometric or elongated shapes. Larger pyrite clasts are cracked and the cracks are filled with blocky calcite cement. Locally, pyrite may occur as fine (0.2 - 0.5 mm across), irregular clasts or framboids (up to about 0.01 mm across) or may fill molds of mollusc shells (mostly juvenile ammonites and bivalves).

The second main component of pyritic-algal microfacies are calcareous algae, mostly representatives of the Rhodophyceae and Porostromata. They occur as rounded fragments of diameters less than 2 mm. Finer algal relics (up to 0.5 mm) are usually less well rounded. The remaining grain components are: fine (less than 0.5 mm) bivalve shell debris, single brachiopod shells and some echinoderm plates. Eccentric ooids occur sporadically. All the grains are embedded within blocky calcite cement. Thin (up to 0.05 mm) isopachous rims develop locally on the algal fragments.

DISCUSSION

The results of microfacies analysis allow us to suggest that the studied material originated from several interfingered facies zones of a vast, shallow and prograding carbonate platform (Fig. 3). Due to paucity of material suitable for examination the model shown in Fig. 3 presents only a hypothetic distribution of specific facies, on the carbonate platform slope during the redeposition of sediments into the deeper parts of the basin. This redeposition took place after the sedimentation of most of the distinguished types of platform sediments. Only the ooids and simple oncoids undoubtly formed during the deposition of conglomerate layers (Berriasian). The other facies constituents could result from the erosion of older carbonate platform sediments (Lower Berriasian or Tithonian?) which emerged during the uplift of the area. This hypothesis is supported by the apparent similarity of the grain composition of the conglomerates from the Cieszyn Beds and some layers of the Klentnice Formation (Oxfordian-Berriasian). This unit resulted from the erosion of the Pavlov carbonate platform which supplied material to the Ždánice-Subsilesian Basin (Eliáš & Eliášová, 1984; Eliáš, 1992). Layers of grey limestones which occur in the upper part of the Klentnice Formation (Tithonian-Berriasian) contain ooids, oncoids, intraclasts and skeletal fragments of shallow-water organisms (bivalves, echinoderms, foraminifers, sponges and algae).

Reconstruction of depositional environments in the areas of the Silesian Ridge and neighbouring Silesian Basin must be preceded by discussion of the following: (i) formation and diagenesis of ooids, (ii) composition of fossil assemblages, (iii) genesis of dolomitization, pyritization and dedolomitization.

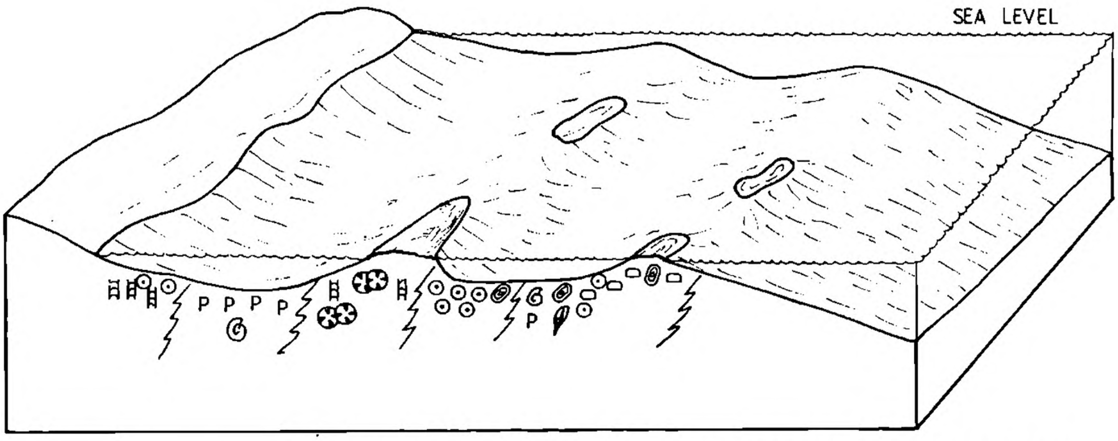

Fig. 3 Hypothetic distribution of facies on carbonate platform of the Silesian Ridge

Hipotetyczny rozkład facji na platformie węglanowej geantykliny śląskiej w tytonie i beriasie

(i) Formation and diagenesis of ooids.

Generally, the ooids were formed in a shallow, high-energy environment. However, differences in both nucleus composition and number of cortical laminae imply depositional environments of variable energy and biocenoses. When the nuclei contain fine shell detritus the cortices comprise numerous laminae. Such ooids are the largest forms. These features indicate an active water enviroment and ooid formation proceeding in nearly permanent suspension. Ooids with the nuclei composed of algae or pelmicrite clasts show a low number of laminae and are of smaller size. This seems to be related either to a less active, presumably deeper-water, environment or to depositional site behind the barrier which separated the zone of flourishing algal growth from an extremely high-energy environment.

Micritization of ooids seems to be related in time to the dissolution of aragonite and formation of pyrite. It is suggested that micritization of ooids proceeded simultaneously with dissolution of aragonitic shells of ammonites, some bivalves and gastropods as well as aragonitic cement which probably filled some interstices between ooids. The internal structure of ooids indicates that micritization was not an affect of the replacement of primary aragonite by calcite but rather resulted from the action of endolithic organisms. These processes were especially intense in the conditions of strongest meteoric influence, i.e. during subaerial exposure (Sellwood & Beckett, 1991).

Authigenic quartz which was encountered in both the nuclei and the cortices, is probably related to late diagenesis (Peszat, 1959).

(ii) Composition of fossil assemblages.

The presence representatives of both the Rhodophyceae and the Porostromata indicates a very shallow-water environment. Rhodophytes seem to be associated with reef-type limestones (Golonka, 1970, 1978) where they could contribute to the reef framework, whereas porostromatans dominated in shallow, back-reef lagoons (Flügel, 1979).

The controversial *Tubiphytes* sp. classified by the authors as oncoids may form specific carbonate buildups with rigid framework (Pomoni-Papaioannou *et al.*, 1989; Matyszkiewicz & Felisiak, 1992). It seems that in Jurassic time these organisms preferred shallow-water environments with limited circulation (Flügel, 1979).

Faunas in the studied samples are represented by an assemblage typical of the so-called "cyanobacterial-sponge facies" (siliceous sponges, polychaetes, small brachiopods). Other members of the assemblage are gastropods, hydrozoans, corals, robust bivalves and piritized, juvenile ammonites. Except for the ammonites, the assemblage undoubtly suggest a shallow-water environment. It must be emphasized that juvenile ammonites were described from so-called "Tubiphytes-reef" (Matyszkiewicz & Felisiak, 1992), which provided perfect refuge for young and probably ill individuals (A. Zeiss, 1992; personal communication).

The depositional depth of the cyanobacterial-sponge facies is disputed. During their formation, water depth is assumed to have been between below wave base, near the base of the photic zone and relatively shallow intrashelf basins (discussion in: Keupp *et al.*, 1990; Leinfelder, 1993). Numerous pertographic features indicating probable episodic emergence of some buildups (Koch & Schorr, 1986; Matyszkiewicz, 1989; Meder, 1989; Liedmann & Koch, 1990; Matyszkiewicz & Felisiak, 1992) are still controversely discussed (Keupp *et al.*, 1990; Selg & Wagenplast, 1990), and suggests more possibilities for their origin than just occasionally exposure.

(iii) Genesis of dolomitization, pyritization and dedolomitization

Dolomitization observed in the studied samples, especially in the case of cavity fillings in the cyanobacterial-sponge limestones, is suggested to have taken place after deposition and partial lithification of the rocks, with the participation of fresh waters ("Dorag" model, Badiozamani, 1973). Both the primary open spaces and the vugs produced by initial karstification were subsequently filled with dolomite presumably formed in the mixing zone fresh/sea waters. Large dolomite clasts can be the fragments of either infillings of larger caverns or completely dolomitized limestones. Such dolomites formed immediately over the algal "reef" and are known from the Carpathian foreland as syngenetic or early diagenetic dolomites (the Ropczyce Series; Golonka, 1978).

Pyritization seems to be connected with two different environments. The angular pyrite intraclasts were transported over short distances and redeposited in a sediment dominated by calcareous algae. The pyrite aggregates from the matrix, as well as pyrite which replaces bivalves and ammonites shells, undoubtly precipitated *in situ*. Bacteria contributed to pyritization, as is documented by common sulphide aggregates composed of framboids (Fisher, 1986). Pyrite was formed during early diagenesis, after dolomitization and dissolution of aragonitic shells and cement, but before dedolomitization. The presence of abundant accumulations of vadose silt within the blocky calcite cement and in the open spaces within the cement seems to be related to aragonite dissolution which preceded pyritization. Vadose silt produced by aragonite dissolution and deposited in the open spaces was overgrown by blocky calcite cement during late diagenesis.

Dedolomitization probably occured after a burial episode which resulted in a reducing environment and formation of pyrite. However, the possibility cannot be neglected that such conditions could dominate before burial, in a shallow lagoon with stagnant waters. Redox changes to oxidizing conditions as a consequence of emergence resulted in pyrite oxidation and release of sulphate ions – a necessary component of dedolomitization process (cf. Scholle, 1971). Coexistence of both brownish iron oxides and vadose silt in the same sediment implies that dedolomitization proceeded under meteoric conditions (cf. Purser, 1985).

The presence of partly dedolomitized clasts which are rather poorly resistant to erosion seems to suggest short transport from the source areas.

CARBONATE PLATFORM

Among various models of Jurassic platforms known from the literature, the one which best fits the studied area seems to be the one of a vast, gently inclined terrain with several transverse barriers, which grades into the area of basinal facies (so-called "gently sloping platform", *sensu* Crevello & Harris, 1984). Progradation together with uplift could give rise to the development of shoals in which conditions were favourable for the formation of ooids and oncoids. The results of the microfacies analysis does not itself permit a full reconstruction of the carbonate platform of the Silesian Ridge in latest Jurassic - earliest Cretaceous time. However, it enables the recognition of the types of environments in the area and suggests their distribution during the redeposition of sediments to the deeper parts of the basin (Fig. 3).

Two barriers are assumed to exist in the proposed model (Fig. 3). One located closer to the emergent part of the Silesian Ridge and representing a shallow basin, either devoid of reef structures or including small patch reefs composed mainly of stromatopores with minor corals. The stromatoporoid-coral patch reefs connected with vast ooidal shoals were described for example from Portugal (Leinfelder, 1992; Leinfelder *et al.*, 1993), Spain (Giner & Barnolas, 1979) and the Northern Alps (Steiger & Wurm, 1980). However, the fossil assemblage observed in thin sections suggests that the model barrier was presumably formed by so-called "sponge-coral-algal mounds" similar to those reported from the Jurassic Smackover Formation

(Crevello & Harris, 1984). In this formation the sponge-coral-algal mounds are locally covered by ooidal grainstones, which imply progressive shallowing of the prograding platform. Least probable is an alternative that the model barrier was a narrow, marginal reef built of sponges, corals and algae, and surrounding a large, shallow lagoon. A similar arrangement has been described by Flügel (1979) from Upper Norian reef limestones of the Dachstein Platform (Northern Calcareous Alps). These sediments include numerous reef breccias which are absent from the Cieszyn Limestones. However, the lack of reef talus deposits in the study area may be explained in terms of the development of only the basal part of a reef structure (the so-called "mud mound stadium") which formed at a somewhat greater depth and did not supply reef debris. Such stages of development of a solenoporoid-coral reef were recognized by Senowbari-Daryan & Schafer (1979) in the Rhaetian strata of the Northern Calcareous Alps. Further development of such a structure and its transition to the typical reef stage could be inhibited by the platform progradation or restricted water circulation in the fore-reef area caused by the growth of a deeper barrier.

In the slope-adjacent lagoon (Fig. 3) strong restriction of water circulation, combined with a flourishing biota along the margins, could produce local reducing conditions in the deepest parts of the sub-basin. Undoubtedly, reducing conditions dominated in the buried sediment, just below the water/sediment interface. This was the site of pyritization of plant fragments and shells. Ooids (mostly types 2 and 3) could develop and algae could grow in the nearshore parts of such a lagoon.

The development of both sub-basins in Fig. 3 shifted in time. Initially, a consecutive "quasi-lagoon" located away from the platform slope did not have well-defined boundaries. Hypothetically, it may have been separated from the open sea by a chain of cyanobacterial-sponge buildups which constituted an arbitrary boundary between the platform slope and deeper parts of the basin. Such a position of cyanobacterial-sponge buildups has been reported from numerous fossil carbonate platforms (Mazagan – Steiger & Jansa, 1984; Nova Scotia – Eliuk & Levesque, 1989; Lusitania Basin – Leinfelder, 1992; Leinfelder *et al.*, 1993). The idea that such structures could episodically emerge during growth does not seem to be valid (see Keupp *et al.*, 1990; Selg & Wagenplast, 1990) except for single, isolated buildups (cf. Burchette & Wright, 1992). Emergence and resulting diagenesis of these structures under meteoric conditions proceeded later in their history and were caused by tectonic uplift rather than by growth to sea level (cf. Matyszkiewicz, 1993; Matyszkiewicz, 1994).

Progressing platform progradation along with tectonic uplift resulted in the deeper sub-basin developing as a "quasi-lagoon" Better circulation, especially in front of a poorly developed coral-algal reef (Fig. 3) produced an environment favourable for the formation of ooids (mainly type 1).

PALAEOGEOGRAPHY OF THE SILESIAN BASIN

The Cieszyn Beds were deposited in the geosynclinal Silesian Basin bordered by two tectonic structures: the Inwałd Ridge to the north and the Silesian Ridge (known also as Silesian Island) to the south (Książkiewicz, 1956, 1960; Nowak, 1973; Eliáš & Eliášová, 1984). During Kimmeridgian and late Tithonian time (Lower Cieszyn Shales) the clastic material supplied to the basin originated mostly from the Inwałd Ridge. Pelitic carbonate and clay material was supplemented by fragments of reef limestones and fossils.

Products of submarine mass movements observed in many sequences of the Lower Cieszyn Beds are the manifestations of vertical tectonic displacements within the ridge (Słomka, 1986b) which have commenced in early Tithonian time. Expanding land areas supplied larger volumes of clastic material transported by submarine slides to the basin floor. In late Tithonian time (Upper Cieszyn Limestones) sediments increasingly developed the characteristics of calcareous flysch (Książkiewicz, 1951; Peszat, 1967; Słomka, 1986a). Dominatant sources of detritus were still the islands of the Inwałd Ridge but the influence of the second source area – an island located at the western edge of the Silesian Ridge became more and more important. In the Berriasian time uplift within the Silesian Basin resulted in the formation of two east-west orientated troughs: Goleszów and Wiślica, separated by discontinuous submarine ridge (Fig. 4) (Nowak, 1973; Słomka, 1986a). The Inwałd Ridge, which bordered the Silesian Basin to the north, mostly supplied the Wiślica trough, whereas the islands of the Silesian Ridge provided material for the Goleszów trough (Słomka, 1986a). Several islands on the Inwałd Ridge were subject to extensive denudation and derived clastic material (calcareous pelite and reef limestone fragments) mixed with debris of shallow-water fauna and flora to be deposited by diluted turbidity currents along the foot of the ridge (Peszat, 1967; Książkiewicz, 1971; Słomka, 1986a).

The carbonate platform existed into Late Tithonian time and provided excellent conditions for fluorishing organic life, represented by calcareous algae, sponges, corals, bryozoans, brachiopods, bivalves, ammonites and crinoids. In Late Tithonian time tectonic movements led to emergence of the western edge of the Silesian Ridge (the present-day area of Silesian-Moravian Beskid). Initially, only the highest parts of the carbonate platform were eroded and resulting clastic material was deposited as a rather limited apron parallel to the basin axis (see Mullins & Cook, 1986; Watts & Garrison, 1986). Progressive uplift caused persistent emergence of other fragments of the Silesian Ridge. Permanent supply of large volumes of clastic material deposited in the upper part of the island slope led to localized sedimentation in the Leszna Górna submarine fan (Słomka, 1986a) (Fig. 4). The fan prograded along the slope of the axial zone, i.e. generally eastward. Preserved sequences mainly represent the outer zone. The lack of inner zone and poorly represented central zone, together with transport directions constrained by the basin inclin-

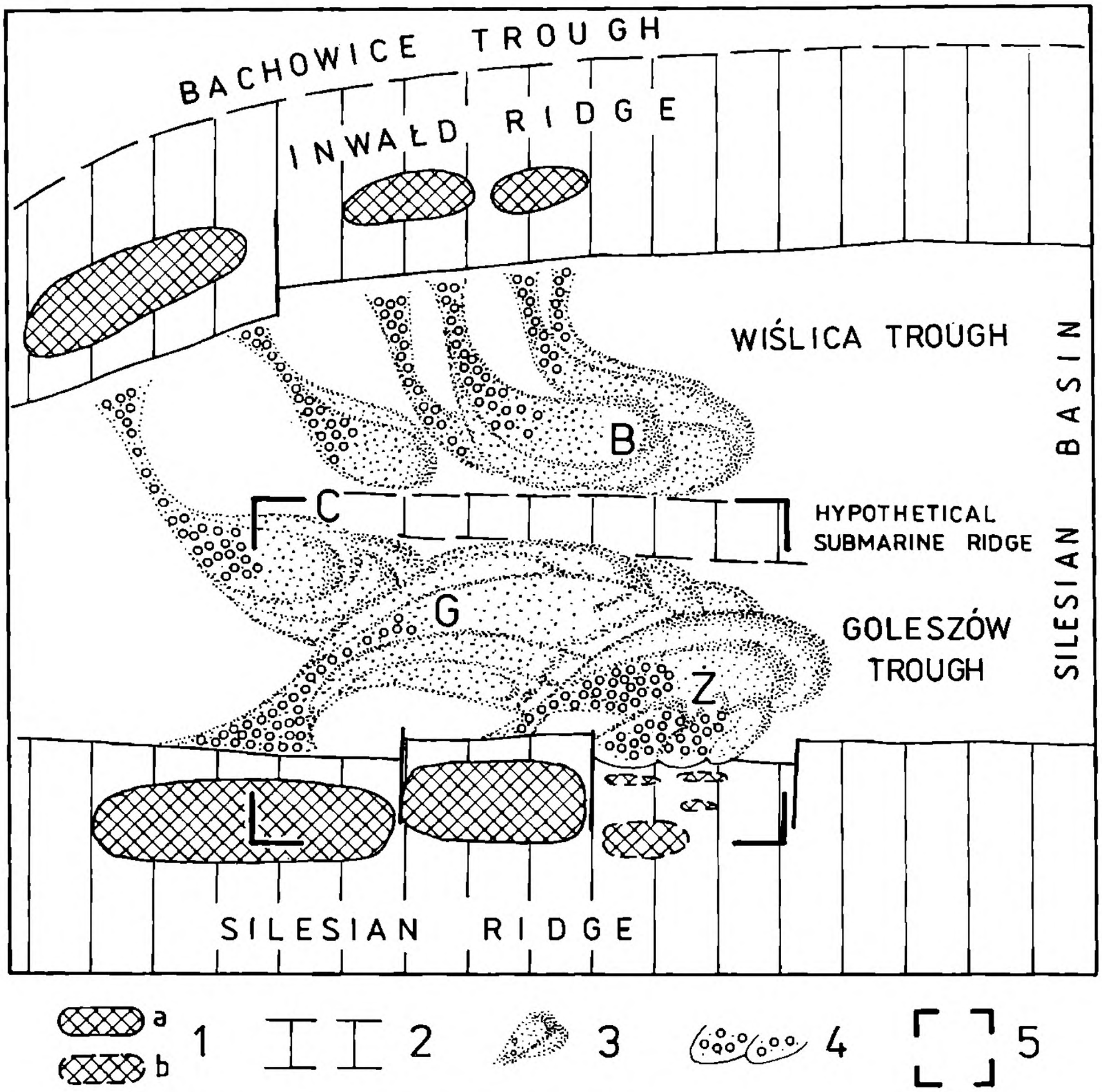

Fig. 4 Berriasian palaeogeography of the Silesian Basin. *1* – islands: *a* – emerged at least since Tithonian; *b* – emerged in Berriasian; *2* – submarine ridges, *3* – submarine fans; *4* – slope apron; *5* – fragment shown in Fig. 5, B – Bielsko-Biała, C – Cieszyn, G – Goleszów

Paleogeografia basenu śląskiego w beriasie. *1* – wyspy: *a* – wynurzone co najmniej od tytonu; *b* – wynurzone w beriasie; *2* – grzbiety podwodne; *3* – stożki podmorskie; *4* – utwory fartucha; *5* – fragment przedstawiony na fig. 5; B – Bielsko-Biała; C – Cieszyn; G – Goleszów

tion, allow one to conclude that the source areas for the clastic material were located exclusively along the Inwałd Ridge (Peszat, 1967; Książkiewicz, 1971; Malik, 1986). However, such a scheme is inconsistent with the facies distribution in the basin. The greatest thicknesses of coarse-grained and thick-bedded facies (conglomerates, coarse-detrital limestones) are located in the southwestern part of the basin (Peszat, 1967, Menčik et al., 1983; Malik, 1986), i.e. they are most distant from the construed source areas. Furthermore, apart from the dominatant eastward and southeastward transport directions

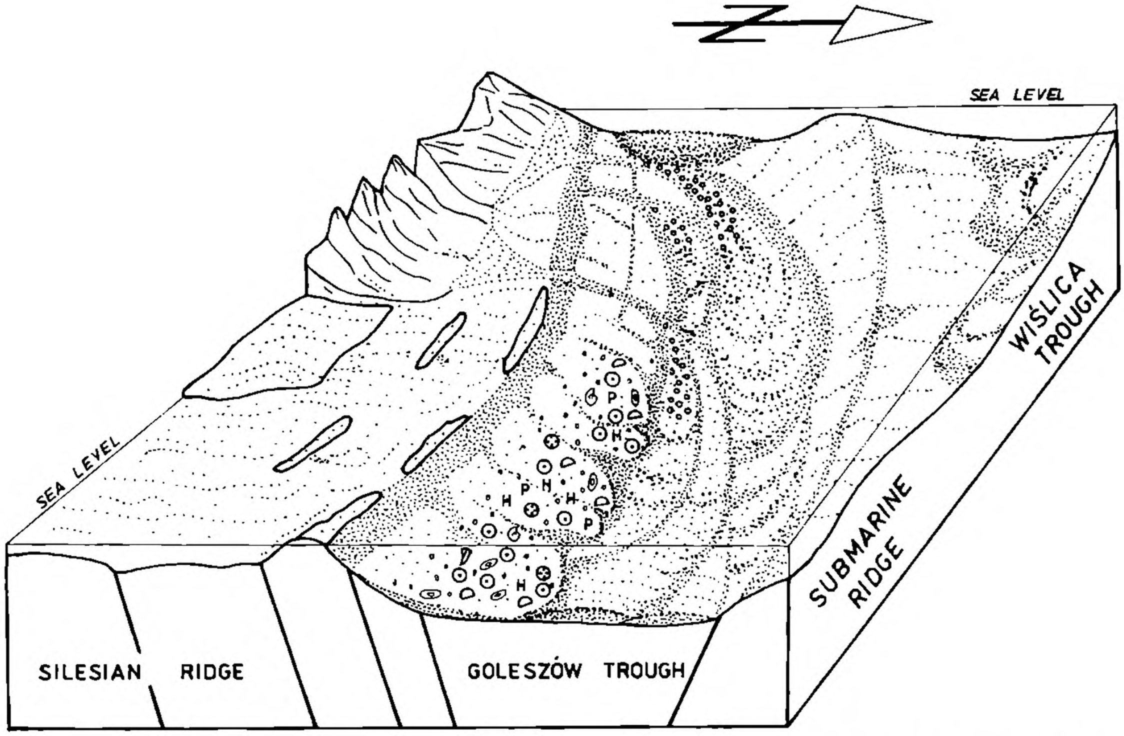

Fig. 5 Blockdiagram illustrating the genesis of organodetrital limestones with ooids. Explanations as in Fig. 3 and 4

Blokdiagram ilustrujący genezę ławic zlepieńców organodetrytycznych z ooidami. Objaśnienia jak na Fig. 3 i 4

proved by Książkiewicz (1962), Peszat (1967), Ślączka *et al.* (1976), and Malik (1986), other possibilities have also been mentioned by these authors (i.e. northeastward). Finally, Słomka (1986a) also suggested the role of northern transport direction in deposition of there coarse grained facies.

Interpretation of the results of microfacies analysis of limestone conglomerates from Żywiec area allowed us to make a attempt at the reconstruction of the Silesian Ridge carbonate platform preliminary in latest Jurassic to earliest Cretaceous time. These results support the hypothesis of the existence of emerged parts of this ridge as early as in Tithonian time (see Książkiewicz, 1951; Nowak, 1973; Słomka, 1986a, Krobicki, 1993) and prove the gradual eastward migration of tectonic movements which successively uplifted tectonic blocks of the ridge (Fig. 5). Intense uplifts within the Silesian Ridge are also documented by the sediments of debris-mud flows reported from the Soła sequence by Książkiewicz (1958). Although this author attributed the flows to the Upper Cieszyn Shales (Valanginian), at least some of these structures undoubtly occur within the Upper Cieszyn Limestones (Słomka, 1993). Therefore, a pattern can be established in the denudation of uplifted blocks and deposition of resulting clastic material. During the initial destruction of carbonate platform, deposition took place in the rather chaotic form of an apron.

Subsequently, sedimentation became more ordered in the form of a submarine fan. Eastward migration of uplift led to lateral interfingering of both types of deposition. The submarine fan formed at the foot of the early uplifted western block of the Silesian Ridge whereas an apron developed along the edges of the newly uplifted eastern block (Fig. 5). An intensively eroded, emerged fragment of the Silesian Ridge supplied clastic material which migrated downslope and became enriched in components of the contemporaneous shallow-water sediments.

Acknowledgements

Thanks are due to Professors Aleksandra Kostecka and Janusz Kotlarczyk for critical reading and valuable discussion. The authors are very much indebted to Dr. M. Hoffman for his criticism and suggestions which significantly improved the manuscript. Finally, discussions with Dr. Michał Krobicki and drawings prepared by Mr. Jan Kępiński are appreciated. The authors thanks Dr. Simon Tull for critical reading and lingual support.

REFERENCES

Andrews, J. E., 1986. Microfacies and geochemistry od Middle Jurassic algal limestones from Scotland. *Sedimentology*, 33: 499 – 520.

Badiozamani, K., 1973. The Dorag dolomitization model - application to the Middle Ordovician of Wisconsin. *J. Sedim. Petrol.*, 43: 465 – 484.

Burchette, T. P. & Wright, V. P., 1992. Carbonate ramp depositional systems. *Sedimentary Geology*, 79: 3 – 57.

Carozzi, A. V., 1957. Contribution a l'etude des proprietes geometriques des oolithes - L'exemple du Grand Lac Sale, Utah, USA. *Inst. Nat. Geneve Bull.*, 58: 1 – 51.

Chafetz, H. S., 1986. Marine peloids: a product of bacterially induced precipitation of calcite. *J. Sedim. Petrol.*, 56: 812 – 817.

Crevello, P. D. & Harris, P., 1984. Depositional models for Jurassic reefal buildups. GCS-SEPM. Found. *3rd Ann. Res. Conf., Proc.*: 57 – 102.

Dragastan, O., 1985. Review of Tethyan Mesozoic Algae of Romania. In: Toomey, D. F. & Nitecki, M. N. (eds.), *Palaeoalgology: Contemporary Research and Applications*. Springer, Berlin: 100 – 161.

Eliáš, M., 1970. Lithology and sedimentology of the Silesian unit in the Moravo-Silesian Beskydy Mts. (with English summary). *Sbor. Geol. Ved*, R.G., 18: 7 – 99.

Eliáš, M., 1992. Sedimentology of the Klennice Formation and the Ernstbrunn Limestone (Ždánice - Subsilesian unit of the Outer West Carpathians). *Vest. Cesk. Geol. Ust.*, 67 (3): 179 – 193.

Eliáš, M. & Eliášová, H., 1984. Facies and paleogeography of the Jurassic in the western part of the Outer Flysch Carpathians in Czechoslovakia. *Sbor. Geol. Ved*, Geol., 39: 105 – 170.

Eliuk, E. & Levesque, R., 1989. Earliest Cretaceous sponge reef mounds, Nova Scotia Shelf (Shell Demascota G-32). In: Geldsetzer, H. H. J., James, N. P. & Tebbutt G. E. (eds.): Reef Canada and adjacent areas. *Canad. Soc. of Petrol. Geol., Mem.*, 13: 713 – 720.

Fisher, I. St. J., 1986. Pyrite replacement of mollusc shells from the Lower Oxford Clay (Jurassic) of England. *Sedimentology*, 33: 575 – 585.

Flügel, E., 1979. Paleoecology and microfacies of Permian, Triassic and Jurassic algal communities of platform and reef carbonates from the Alps. *Bull. Centres Rech. Explor. - Prod. Elf-Aquitaine*, 3: 569 – 587.

Gąsiewicz, A., 1984. Eccentric ooids. *Neues Jb. Geol. Paläont. Abh.*,1984: 204 – 211.
Giner, J. & Barnolas, A., 1979. Las construcciones Arrecifales del Jurasico Superior de la Sierra de Albarracin (Teruel). *Cuad. Geol.*, 10: 73 – 82.
Golonka, J., 1970. Calcareous algae from the Upper Jurassic of the Southern periphery of the Świętokrzyskie Mts. *Bull. Acad. Pol. Sc. Ser. Sc. geol. geogr.*, 18, part I: 75 – 84, part II: 85 – 93.
Golonka, 1978. Upper Jurassic microfacies in the Carpathian Foreland (with Polish summary). *Biul. Inst. Geol.*, 310: 5 – 38.
Hohenneger, L., 1861. *Geognostische Karte der Nord-Karpathen in Schlesien und den angrenzenden Theilen von Mähren und Galizien.* Gotha: 50 pp.
Keupp, H., Koch, R. & Leinfelder, R., 1990. Steuerungsprozesse der Entwicklung von Oberjura - Spongiolithen Süddeutschlands: Kenntnisstand, Probleme und Perspektiven. *Facies*, 23: 141 – 174.
Koch, R. & Schorr, M., 1986. Diagenesis of Upper Jurassic sponge-algal reefs in SW Germany. In: Schroeder, J. H. & Purser, B. H. (eds.): *Reef diagenesis*. Springer, Berlin: 224 – 244.
Krobicki, M., 1993. Tithonian-Berriasian brachiopods in the Niedzica Succession of the Pieniny Klippen Belt (Polish Carpathians): paleoecological and paleobiogeographical implications. In: Palfy, J. & Vörös A. (eds.), *Mesozoic Brachiopods of Alpine Europe. Hung. Geol. Soc.*: 69 – 77.
Książkiewicz, M., 1951. *Objaśnienie do arkusza Wadowice.* Państw. Inst. Geol., Warszawa: 272 pp.
Książkiewicz, M., 1956. Geology of the Northern Carpathians. *Geol. Rundsch.*, 45: 369 – 411.
Książkiewicz, M., 1958. Submarine slumping in the Carpathian Flysch. *Roczn. Pol. Tow. Geol.*, 28: 123 – 150.
Książkiewicz, M., 1960. Outline of the palaeogeography in the Polish Flysch Carpathians. *Prace Inst. Geol.*, 30 (2): 236 – 249.
Książkiewicz, M. (ed.), 1962. *Geological atlas of Poland. Fasc.13: Cretaceous and Early Tertiary in the Polish External Carpathians.* Wyd. Geol., Warszawa.
Książkiewicz, M., 1971. On the origin of the Cieszyn Limestones in the Carpathian Flysch. *Bull. Acad. Pol. Sci., Ser. geol.*, 19 (3): 131 – 136.
Leinfelder, R. R., 1992. A modern-type Kimmeridgian reef (Ota Limestone, Portugal): implications for Jurassic reef models. *Facies*, 26: 11 – 34.
Leinfelder, R. R., 1993. Upper Jurassic reef types and controlling factors. *Profil*, 5: 1 – 45.
Leinfelder, R. R., Krautter, M., Nose, M., Ramalho, M., M. & Werner, W., 1993. Siliceous sponge facies from the Upper Jurassic of Portugal. *Neues Jb. Geol. Paläont. Abh.*, 189: 199 – 254.
Liedmann, W. & Koch, R., 1990. Diagenesis and fluid inclusions of Upper Jurassic sponge-algal reefs in SW Germany. *Facies*, 23: 241 – 268.
Malik, K., 1986. Turbidite facies and fan-facies associations in the Cieszyn Limestones (Upper Tithonian - Berriasian, Northwestern Carpathians, Poland). In: Teisseyre, A. K. (ed.): *7th European Regional Meeting Excursion Guidebook* Kraków-Poland. Ossolineum, Wrocław: 53 – 66.
Maslov, V. P., 1956. Iskopaemye izvestkovye vodorosli SSSR. *Trudy Geol. Inst. AN SSSR*, 160: 1 – 301.
Matyszkiewicz, J., 1989. Sedimentation and diagenesis of the Upper Oxfordian cyanobacterial-sponge limestones in Piekary near Kraków. *Ann. Soc. Geol. Polon.*, 59: 201 – 231.
Matyszkiewicz, J., 1993. Genesis of stromatactis in an Upper Jurassic Carbonate Buildup (Młynka, Cracow Region, Southern Poland): Internal reworking and erosion of organic growth cavities. *Facies*, 28: 87 – 96.
Matyszkiewicz, J., 1994. Remarks on the deposition and diagenesis of the pseudonodular limestone in the Cracow area (Oxfordian; Southern Poland). *Berliner geow. Abh.*, 13: 419 – 439.
Matyszkiewicz, J. & Felisiak, I., 1992. Microfacies and diagenesis of an Upper Oxfordian carbonate buildup in Mydlniki (Cracow area, Southern Poland). *Facies*, 27: 179 – 190.
Meder, K., 1989: Mikrofazies und Diagenese der Karbonatgesteine des höheren Malm (ki 2.4 - ti H) in der Bohrung Saulgau GB 3. *Abh. geol. Landesamt Bad.-Württ.*, 13: 89 – 137.
Menčik et al., 1983. Geology of the Moravskoslezské Beskydy Mts. and Podbeskydská pahorkatina Upland (with English summary). *Ustredni Ustav Geologicky*. Praha: 304 pp.

Mišik, M., 1974. Paleogeographic outline of the Tithonian in the Czechoslovakian Carpathians. *Acta Geol. Polon.*, 24 (3): 485 – 503.

Morycowa, E. & Moryc, W. 1976. The Upper Jurassic sediments in the foreland of the Polish Carpathians (Sandomierz Basin). (with Polish summary). *Rocz. Pol. Tow. Geol.*, 46: 231 – 288.

Mullins, H. T. & Cook, H. E., 1986. Carbonate apron models: alternatives to the submarine fan model for paleoenvironmental analysis and hydrocarbon exploration. *Sedimentary Geology*, 48: 37 – 79.

Nowak, J., 1927. Esquisse de la téctonique de la Pologne (in Polish with French summary). *Kom. Org. II ZSGE*, Kraków: 160 pp.

Nowak, W., 1966. *Szczegółowa Mapa Geologiczna Polski. 1:50000. Arkusz Bielsko-Biała.* Wyd. Geol., Warszawa.

Nowak, W., 1973. Jura Karpat zewnętrznych. In: Sokołowski, S. (ed.), *Budowa geologiczna Polski*, 1(2), (in Polish only). Wyd. Geol., Warszawa: 389 – 401, 464 – 467.

Peszat, C., 1959. Silicification of Cieszyn Limestones at Leszna Górna near Cieszyn - Western Carpathians. (with english summary). *Kwart. Geol.*, 3 (4): 965 – 976.

Peszat, C., 1967. The lithological development and conditions of sedimentation of the Cieszyn Limestones (with English summary). *Prace Geol. Oddz. PAN w Krakowie*, 44: 1 – 111.

Pomoni-Pappaioannou, F., Flügel, E. & Koch, R., 1989. Depositional environments and diagenesis of Upper Jurassic subsurface sponge- and *Tubiphytes*-reef limestones: Altensteig 1 well, Western Molasse Basin. *Facies*, 21: 263 – 284.

Purser, B. H., 1985. Dedolomite porosity and reservoir properties of Middle Jurassic carbonates in the Paris Basin, France. In: Roehl, P.O. & Choquette, P. W. (eds.), *Carbonate petroleum reservoir*, Springer, Berlin, 343 – 355.

Richter, D. K., 1976. Gravitativer Meniskuszement in einem holozönen Oolith bei Neapolis (Süd-Peloponnes, Griechenland). *Neues Jb. Geol. Paläont. Abh.*, 151: 192 – 223.

Richter, D. K., 1983. Calcareous ooids: a synopsis. In: Peryt, T. M. (ed.), *Coated grains*, Springer, Berlin, 71 – 99.

Scholle, P. A., 1971. Diagenesis of deep-water carbonate turbidites, Upper Createaceous, Monte Antolo Flysh, Northern Appenines, Italy. *J. Sedim. Petrol.*, 41: 233 – 250.

Selg, M. & Wagenplast, P., 1990. Beckenarchitektur im süddeutschen Weißen Jura und die Bildung der Schwammriffe. *Jh. geol. Landesamt Baden - Württemberg*, 32: 171 – 206.

Sellwood, B. W. & Beckett, D., 1991. Ooid microfabrics: the origin and distribution of high intra-ooid porosity; Mid-Jurassic reservoirs, S. England. *Sedimentary Geology*, 71: 189 – 193.

Senowbari-Daryan, B. & Schäfer, P., 1979. Distributional patterns of calcareous algae within Upper Triassic patch reef structures of the Northern Calcareous Alps (Salzburg). *Bull. Centres Rech. Explor. - Prod. Elf - Aquitaine*, 3: 811 – 820.

Słomka, T., 1986a. Statistical approach to study of flysch sedimentation - Kimmeridgian-Hauterivian Cieszyn Beds, Polish Outer Carpathians (with English summary). *Ann. Soc. Geol. Polon.*, 56, 277 – 326.

Slomka, T., 1986b. Submarine mass movement deposits in Lower Cieszyn Shales (with English summary). *Zesz. Nauk. AGH. Geologia*, 12 (4): 25 – 35.

Słomka, T., 1993. *Utwory spływów gruzowo-błotnych w wapieniach cieszyńskich (tyton - berias) rejonu Żywca (Polskie Karpaty fliszowe).* Archiwum Zakł. Geol. Og. i Matem. Wydz. Geol., Geofiz. i Ochr. środ. AGH, Kraków.

Steiger, T. & Wurm, D., 1980. Faziesmuster oberjurassischer Platform - Karbonate (Plassen - Kalke, Nördliche Kalkalpen, Steirisches Salzkammergut; Österreich). *Facies*, 2: 241 – 284.

Steiger, T. & Jansa, L. F., 1984. Jurassic limestones of the seaward edge of the Mazagan carbonate platform, nortwest African continental margin, Morocco. *Initial Rep. Deep Sea Drill. Project*, 79: 449 – 491.

Strasser, A., 1986. Ooids in Purbeck limestones (lowermost Cretaceous) of the Swiss and French Jura. *Sedimentology*, 33: 711 – 727.

Strohmenger, C., Dozet, S. & Koch, R., 1987. Diagenesemuster-Stratigraphie: Oolith-Horizonte im Jura von SW-Slowenien. *Facies*, 17: 253 – 266.

Ślączka, A. (ed.), 1976. *Atlas of palaeotransport of detrital sediments in the Carpathian - Balkan mountain system. Part I: Tithonian - Lower Cretaceous*. Wyd. Geol. Warszawa.
Tokarski, A., 1947. La colline de Grojec et les fenêtres téctoniques de Żywiec (with French summary). *Biul. Państw. Inst. Geol.*, 28: 1 – 72.
Tucker, M. E., 1984. Calcitic, aragonitic and mixed calcitic-aragonitic ooids from the mid-Proterozoic Belt Supergroup, Montana. *Sedimentology*, 31: 627 – 644.
Watts, K. F. & Garrison, R. F., 1986. Sumeini Group, Oman - Evolution of a Mesozoic carbonate slope on a South Tethyan continental margin. *Sedimentary Geolology*, 48: 107 – 168.
Żytko, K., 1966. *Szczegółowa Mapa Geologiczna Polski, 1:50000. Arkusz Milówka*. Wyd. Geol., Warszawa.

Streszczenie

ZLEPIEŃCE ORGANODETRYTYCZNE Z OOIDAMI W WAPIENIACH CIESZYŃSKICH (TYTON - BERIAS) POLSKICH KARPAT FLISZOWYCH I ICH ZNACZENIE PALEOGEOGRAFICZNE

Jacek Matyszkiewicz & Tadeusz Słomka

W wapieniach cieszyńskich górnych (berias) rejonu Żywca, w potoku Leśna stwierdzono występowanie kilku ławic zlepieńców organodetrytycznych z ooidami (Fig. 1, 2). Wyodrębniono w nich następujące mikrofacje: oolitowo-gąbkową, gąbkową i pirytowo-glonową.

Utwory mikrofacji oolitowo-gąbkowej są oosparytami. W składzie ziarnowym dominują ooidy i intraklasty wapieni cyjanobakteryjno-gąbkowych; podrzędnie występują onkoidy, otwornice, hydrozoa i glony. Składniki ziarnowe tkwią w blokowym cemencie kalcytowym. Podstawowym składnikiem mikrofacji gąbkowej są intraklasty wapieni cyjanobakteryjno-gąbkowych z fauną wieloszczetów, serpul, otwornic, drobnych ślimaków i hydrozoa. Matriks tej mikrofacji stanowi głównie blokowy cement kalcytowy, ale obserwuje się także nagromadzenia wadycznego siltu. Utwory mikrofacji pirytowo-glonowej wykształcone są jako grainstone, lokalnie rudstone. Głównymi składnikami są okruchy detrytycznego pirytu i fragmenty glonów (krasnorosty i Porostomata). Wśród pozostałych składników obserwuje się detryt skorup małżów, pojedyncze skorupy ramienionogów, płytki szkarłupni oraz ooidy. Składniki ziarnowe tkwią w blokowym cemencie kalcytowym.

Z analizy mikrofacjalnej wynika, że badany materiał pochodzi z kilku zazębiających się obszarów facjalnych położonych w rejonie płytkiej i progradującej platformy węglanowej. Przedstawiony model (Fig. 3) nie rekonstruuje środowiska sedymentacji, ale ilustruje jedynie hipotetyczne rozmieszczenie poszczególnych facji platformy węglanowej na etapie częściowego jej wynurzenia i redepozycji materiału do głębszych części basenu śląskiego. Jedynie ooidy i onkoidy proste tworzyły się w trakcie depozycji ławic zlepieńców (berias). Pozostałe składniki wyróżnionych facji pochodziły z niszczenia starszych osadów platformowych (niższy berias, tyton?).

W proponowanym modelu założono istnienie dwu barier (Fig. 3). Pierwsza z nich, położona bliżej strefy wynurzonej grzbietu śląskiego była najprawdopodobniej utworzona przez tzw. sponge-coral-algal mounds. W lagunie położonej między strefą wynurzoną a tą barierą silne ograniczenie cyrkulacji wody mogło nawet powodować powstanie lokalnych warunków redukcyjnych w jej najgłębszych partiach. Warunki takie panowały niewątpliwe w osadzie pogrzebanym, tuż poniżej granicy osad/woda, gdzie zachodziły procesy pirytyzacji napławianych roślin i skorup. W partiach brzeżnych tej laguny tworzyły się ooidy i rozwijały glony.

Kolejne przegłębienie usytuowane bliżej skłonu platformy oddzielał pierwotnie od otwartego morza pas budowli cyjanobakteryjno-gąbkowych. Progradacja platformy i tektoniczne ruchy wznoszące spowodowały, że subbasen ten z upływem czasu przejął rolę quasi-laguny. Silniejsza cyrkulacja wody panująca w jej wnętrzu, szczególnie na przedpolu bariery koralowo-glonowej stwarzała dogodne warunki do tworzenia się ooidów.

Warstwy cieszyńskie powstawały w geosynklinalnym basenie śląskim, ograniczonym grzbietami: od północy inwałdzkim, a od południa śląskim. W kimerydzie i wczesnym tytonie (łupki cieszyńskie dolne) dostarczany do basenu materiał okruchowy pochodził głównie z grzbietu inwałdzkiego. W późnym tytonie (wapienie cieszyńskie dolne) tworzyły się osady o coraz wyraźniejszych cechach fliszu wapiennego. Dominujący źródłem materiału był nadal grzbiet inwałdzki, ale stopniowo rósł udział drugiego źródła – wyspy zlokalizowanej na zachodnim krańcu grzbietu śląskiego. W beriasie, wskutek ruchów wypiętrzających w basenie śląskim utworzyły się dwie równoleżnikowe rynny: goleszowska i wiślicka, rozdzielone nieciągłym wałem podmorskim (Fig. 4). Grzbiet inwałdzki zasilał rynnę wiślicką, natomiast rynnę goleszowską głównie wyspy grzbietu śląskiego. Na grzbiecie śląskim aż do późnego tytonu rozwinięta była platforma węglanowa z bujnie rozwijającym się życiem organicznym. W późnym tytonie ruchy wypiętrzające doprowadziły do wynurzenia zachodniego krańca grzbietu. Początkowo powstający materiał okruchowy usypywany był w formie niezbyt rozległego fartucha równolegle do osi basenu. Postępujące ruchy wypiętrzające trwale wynurzyły większe fragmenty grzbietu śląskiego, a ustabilizowana dostawa dużych ilości materiału okruchowego gromadzonego w górnej części skłonu wyspy doprowadziła do skanalizowania depozycji w formie podmorskiego stożka napływowego (Fig. 5). Progradacja tego stożka następowała w kierunku nachylenia strefy osiowej, a więc generalnie w kierunku wschodnim.

W procesie niszczenia wynurzanych bloków i sedymentacji powstającego materiału okruchowego zaznaczyła się prawidłowość. Początkowo, w trakcie niszczenia platformy węglanowej, depozycja odbywała się w obrębie chaotycznie usypywanego fartucha, a później następowało uporządkowanie sedymentacji w formie głębokomorskiego stożka. Przesuwanie się ruchów wypiętrzających na wschód doprowadziło do bocznego zazębiania się tych dwóch typów sedymentacji. Podmorski stożek usypywany był u podnóża wcześniej wypiętrzonego, usytuowanego na zachodnim krańcu, bloku grzbietu śląskiego, zaś fartuch wzdłuż świeżo wypiętrzanego wschodniego bloku, w trakcie niszczenia platformy węglanowej (Fig. 5).

Interpretacja badań mikrofacjalnych zlepieńców wapiennych z rejonu Żywca umożliwia pierwszą próbę rekonstrukcji budowy platformy węglanowej grzbietu śląskiego na przełomie jury i kredy. Potwierdza także hipotezę o istnieniu stref wynurzonych, w obrębie tego grzbietu, już w tytonie, oraz dokumentuje fakt stopniowego przesuwania się na wschód ruchów wypiętrzających kolejne bloki tektoniczne tego grzbietu.

EXPLANATIONS OF PLATES (OBJAŚNIENIA PLANSZ)

Plate (Plansza) I

1 — Type 1 ooid. Numerous, well-developed microspar laminae separated by micrite envelopes grow concentrically on the nucleus. The nucleus is partly silicified. On the left - fragment of algae *Marinella lugeoni* Pfender. Oolithic-sponge microfacies.

Ooid typu 1. Widoczne liczne, dobrze czytelne powłoki mikrosparu przedzielone międzypowłokami mikrytowymi i rozwinięte koncentrycznie na jądrze. Jądro częściowo zsylifikowane. Z lewej fragment glonu *Marinella lugeoni* Pfender. Facja oolitowo-gąbkowa.

2 — Type 1 ooid. Nucleus is a pelmicrite intraclast with abundant authigenic quartz crystals. Microspar laminae are well developed only in the areas of maximum curvature. Oolithic-sponge microfacies.

Ooid typu 1. Jądro tworzy intraklast pelmikrytowy z licznymi kryształami kwarcu autigenicznego. Mikrosparytowe laminy są wyraźnie rozwinięte jedynie na odcinkach największej krzywizny jądra. Facja oolitowo-gąbkowa.

3, 4 — Type 1 ooids. Nuclei are silicified and authigenic quartz crystals are produced. Oolithic-sponge microfacies.

Ooidy typu 1. Jądra wykazują sylifikację kwarcem autigenicznym. Facja oolitowo-gąbkowa.

Plate (Plansza) II

1 — Type 1, 3 and 4 ooids. Central left - type 1 ooid with numerous, well-preserved laminae coexists with type 3 ooids (bottom left, top right) which show poorly developed cortex with few laminae growing over a large nucleus and with type 4 (bottom right) ones which have only one laminae composed of radially arranged crystals. Oolithic-sponge microfacies.

Ooidy typu 1, 3 i 4. Ooid typu 1 (z lewej, w środku) o licznych i dobrze czytelnych powłokach korteksu współwystępuje z ooidami typu 3 (z lewej, u dołu; z prawej, u góry), które cechuje słabo rozwinięty korteks zbudowany z nielicznych lamin otaczających duże jądro i ooidami typu 4 (z prawej, u dołu) charakteryzujących się korteksem zbudowanym z jednej laminy utworzonej z radialnie ułożonych krzyształów. Facja oolitowo-gąbkowa.

2 — Type 3 ooid. Poorly developed cortex grows around nucleus which is partly micritized echinoderm plate. Sponge microfacies.

Ooid typu 3. Widoczny słabo rozwinięty korteks na jądrze, które stanowi płytka szkarłupni częściowo zmikrytyzowana. Facja gąbkowa.

3 — Type 3 ooid (top) and oncoid (bottom). Ooid nucleus is a fragment of algae *Cayeuxia* sp. overgrown by few microsparite envelops. High nucleus/cortex ratio is remarkable. Outer ooid laminae show traces of dissolution along the contact with the oncoid. Dissolved parts are replaced with blocky calcite cement and authigenic quartz. Oncoid (*Tubiphytes* sp.) shows visible concentric structure. The nucleus is formed by foraminifera *Nodophthalmium* sp., the outer laminae are locally intensively dissolved. Oolithic-sponge microfacies.

Ooid typu 3 (u góry) i onkoid (u dołu). Jądro ooidu stanowi fragment glonu cf. *Cayeuxia* sp., na którym rozwinięte są nieliczne powłoki mikrosparu. Zwraca uwagę duży stosunek wielkości jądra do grubości powłok korteksu. Na kontakcie z onkoidem zewnętrzne powłoki korteksu wykazują ślady rozpuszczania. Na miejscu rozpuszczonych fragmentów korteksu występuje blokowy cement kalcytowy i kwarc autigeniczny. Onkoid (typu *Tubiphytes* sp.) wykazuje dość wyraźną koncentryczną budowę; jego jądro buduje przypuszczalnie otwornica cf. *Nodophthalmidium* sp.; zewnętrzne powłoki korteksu są lokalnie silnie rozpuszczone. Facja oolitowo-gąbkowa.

4 — Type 2 ooid. Micritic matrix which encloses the ooid is an infilling of bivalve shell. Boundaries of sparite laminae are obliterated by micritization. Nucleus is poorely pronounced and grades into partly micritized cortex. Oolithic-sponge microfacies.

Ooid typu 2. Mikrytowe matriks otaczające ooid jest wypełnieniem muszli małża. Granice lamin sparytowych są zatarte w następstwie zaawansowanej mikrytyzacji. Jądro jest słabo wyodrębnione i płynnie przechodzi w zmikrytyzowany częściowo korteks. Facja oolitowo-gąbkowa.

5 — Simple oncoids. One of the oncoids in the centre of photograph shows nucleus composed of partly dissolved gastropod shell. In bottom part - foraminifera *Ammobaculites* sp. Oolithic-sponge microfacies.

Onkoidy proste. W środku zdjęcia jądrem jednego z onkoidów jest częściowo rozpuszczona muszla ślimaka. U dołu otwornica *Ammobaculites* sp. Facja oolitowo-gąbkowa.

Plate (Plansza) III

1 — Type 3 ooids embedded in pyritic matrix. Relics of aragonite rods locally grow on the outer surfaces of the grains. Some of the relics show features of meniscus cement. Pyritic matrix is locally composed spherulitic aggregates. Sponge microfacies.

Ooidy typu 3 występujące w obrębie pirytowego matriks. Na zewnętrznych powłokach ooidów występują lokalnie igiełkowate relikty kryształów aragonitu. Lokalnie relikty te mają charakter cementu meniskowego. Pirytowe matriks jest lokalnie zbudowane z agregatów składających się z licznych kuleczek. Facja gąbkowa.

2 — Type 2 ooids. Very regular shape of the grain is remarkable. Laminae boundaries are obliterated by advanced micritization. Nucleus is poorely defined. Locally, authigenic quartz crystals can be observed in cortex and in cracks. Oolithic-sponge microfacies.

Ooid typu 2. Zwraca uwagę bardzo regularny kształt ziarna. Granice poszczególnych lamin są zatarte w wyniku zaawansowanej mikrytyzacji. Jądro jest bardzo słabo wyodrębnione. Lokalnie, w obrębie korteksu oraz w szczelinach spękań widoczne liczne kryształy kwarcu autigenicznego. Facja oolitowo-gąbkowa.

3 — Type 3 ooids. Nucleus composed of echinoid spine is overgrown by partly micritized microspar laminae. Oolithic-sponge microfacies.

Ooid typu 3. Jądro stanowi kolec jeżowca, na którym rozwinięte są powłoki mikrosparu, częściowo zmikrytyzowane. Facja oolitowo-gąbkowa.

4 — Type 1 and 3 ooids forming aggregate grains. Fragment of algae *Marinella lugeoni* Pfender visible on the right. Oolithic-sponge microfacies.

Ooidy typu 1 i 3 mogą występować w formie ziarn agregacyjnych. Z prawej fragment glonu *Marinella lugeoni* Pfender. Facja oolitowo-gąbkowa.

Plate (Plansza) IV

1 — Partly deformed type 3 ooid (left) and eccentric type 5 ooid (right). Oolithic-sponge microfacies.

Częściowo zdeformowany ooid typu 3 (z lewej) i ooid ekscentryczny typu 5 (z prawej). Facja oolitowo-gąbkowa.

2 — Ooids in pyritic matrix. Sponge microfacies.

Ooidy w pirytowym matriks. Facja gąbkowa.

3 — Strongly micritized ooids with nuclei replaced by authigenic quartz grains with numerous inclusions. Sponge microfacies.

Silnie zmikrytyzowane ooidy o jądrach zastąpionych przez kwarc autigeniczny zawierający liczne inkluzje. Facja gąbkowa.

4 — Oncoid *Tubiphytes* sp. Outer laminae are locally dissolved. Cortex encloses numerous authigenic quartz crystals. Oolithic-sponge microfacies.

Onkoid typu *Tubiphytes* sp. Zewnętrzne powłoki korteksu są lokalnie rozpuszczone. Korteks zawiera liczne kryształy kwarcu autigenicznego. Facja oolitowo-gąbkowa.

Plate (Plansza) V

1 — Fragment of calcareous algae *Solenopora* sp. Oolithic-sponge microfacies.

Fragment glonu wapiennego *Solenopora* sp. Facja oolitowo-gąbkowa.

2 — Fragment of calcareous algae *Solenopora* sp., section close to transversal. Pyritic-sponge microfacies.

Fragment glonu wapiennego *Solenopora* sp., przekrój zbliżony do poprzecznego. Facja pirytowo-glonowa.

3 — Fragment of calcareous algae *Cayeuxia* sp. Pyritic-sponge microfacies.

Fragment glonu wapiennego *Cayeuxia* sp. Facja pirytowo-glonowa.

4 — Fragment of algae filament *Marinella lugeoni* Pfender. Sponge microfacies.

Fragment plechy glonu *Marinella lugeoni* Pfender. Facja gąbkowa.

5 — Red algae *Marinella lugeoni* Pfender. Pyritic-sponge microfacies.

Krasnorost *Marinella lugeoni* Pfender. Facja pirytowo-glonowa.

Plate (Plansza) VI

1 — Hydrozoans with vadose silt on the left. Sponge microfacies.

Hydrozoa. Z lewej wadyczny silt. Facja gąbkowa.

2 — Longitudial section of a coral with local vadose silt infilling. Sponge microfacies.

Przekrój podłużny przez koralowiec. Lokalnie widoczne wypełnienie wadycznym siltem. Facja gąbkowa.

3 — Transversal section of a coral. Sponge microfacies.

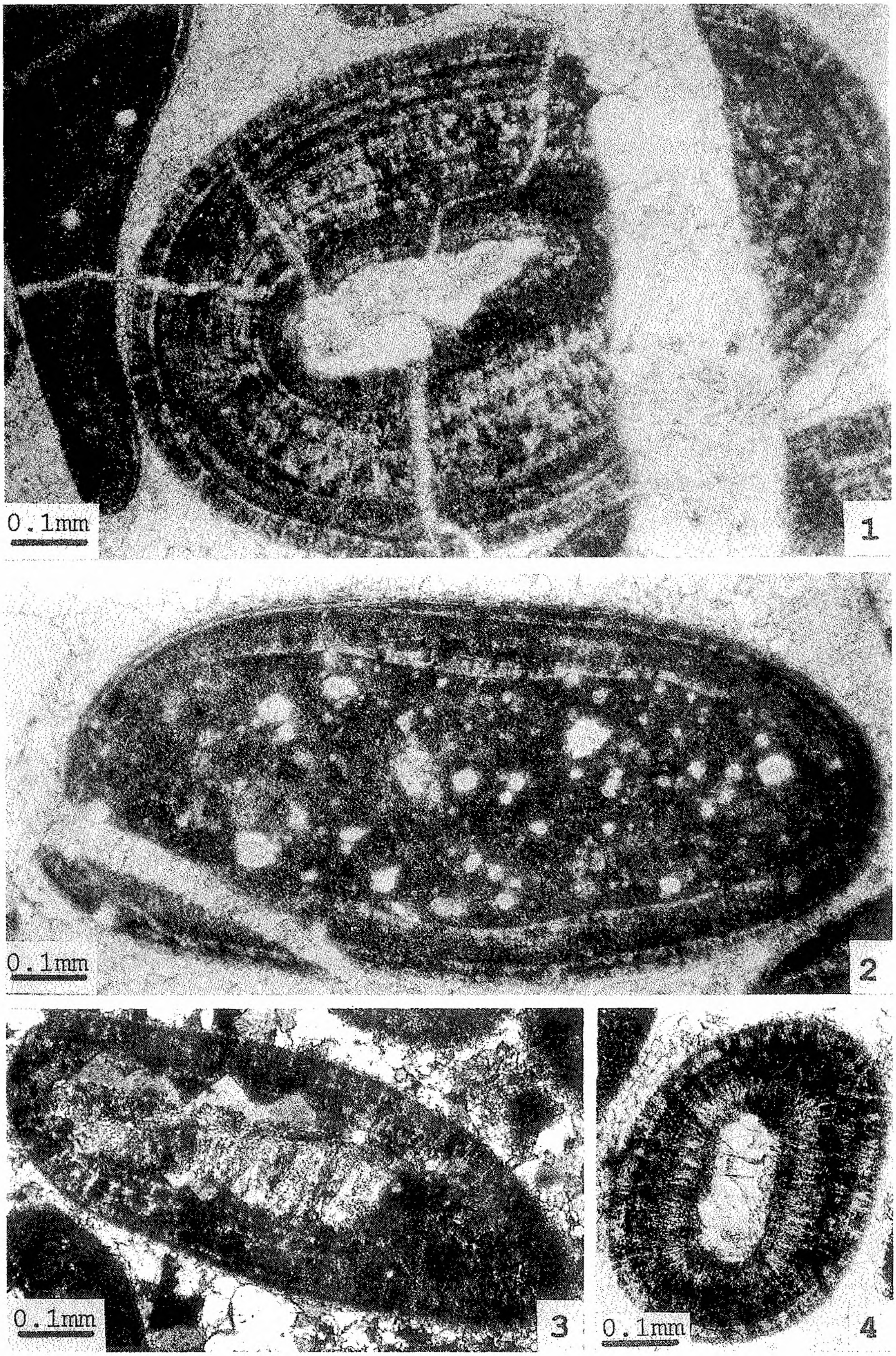
0.1mm
1
0.1mm
2
0.1mm
3
0.1mm
4

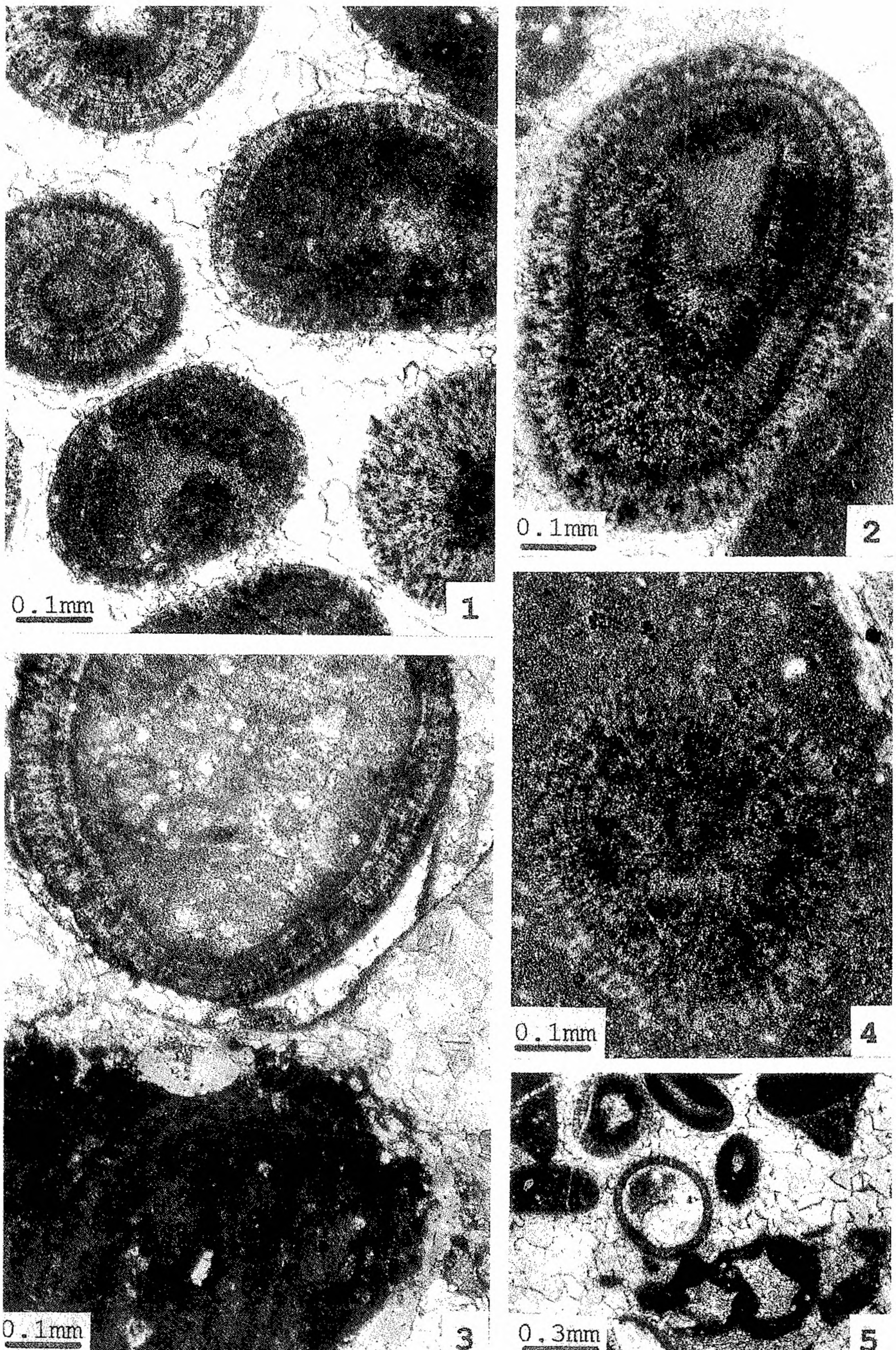
0.1mm
1
0.1mm
2
0.1mm
3
0.1mm
4
0.3mm
5

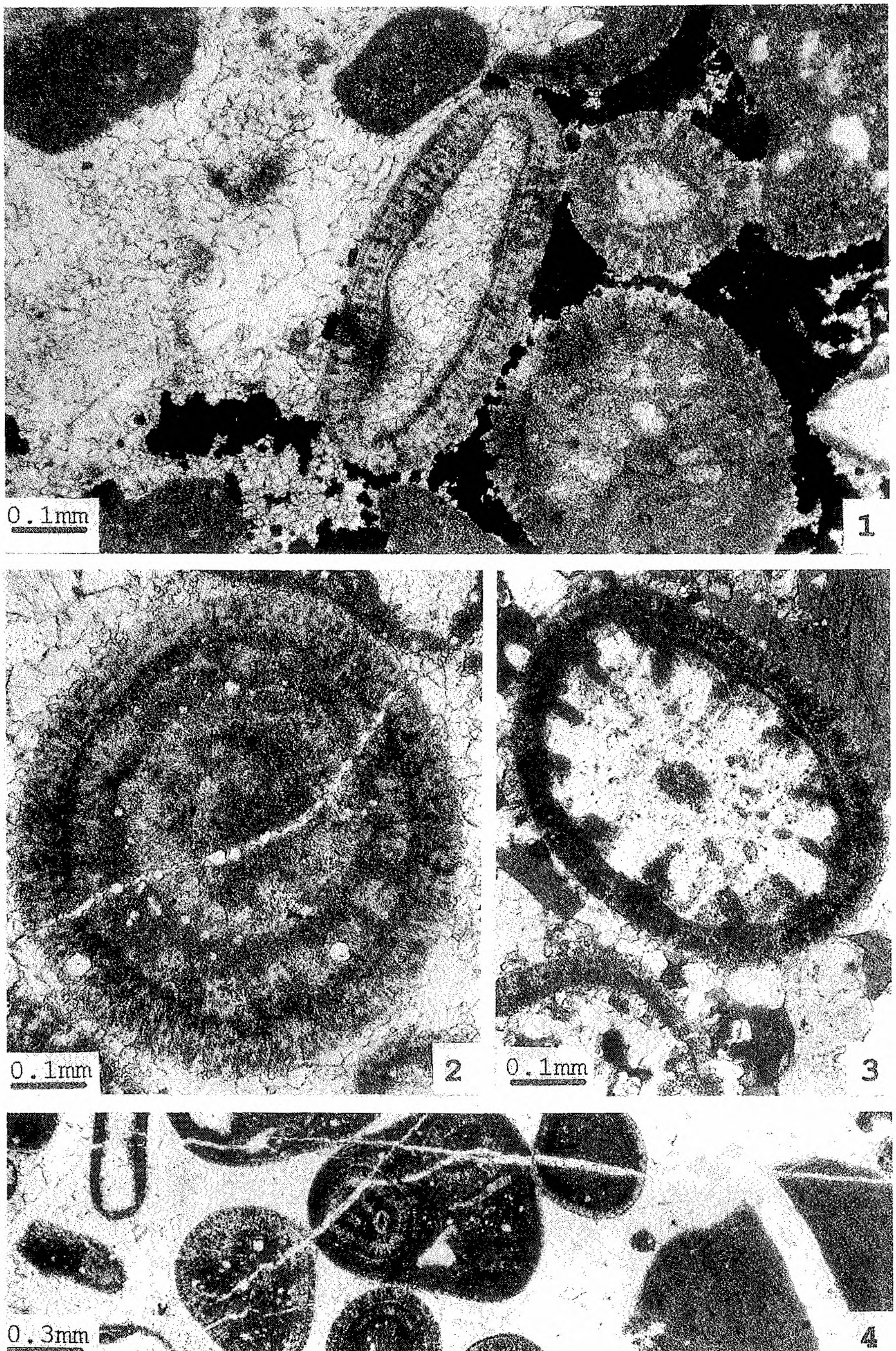
0.1mm
1
0.1mm
2
0.1mm
3
0.3mm
4

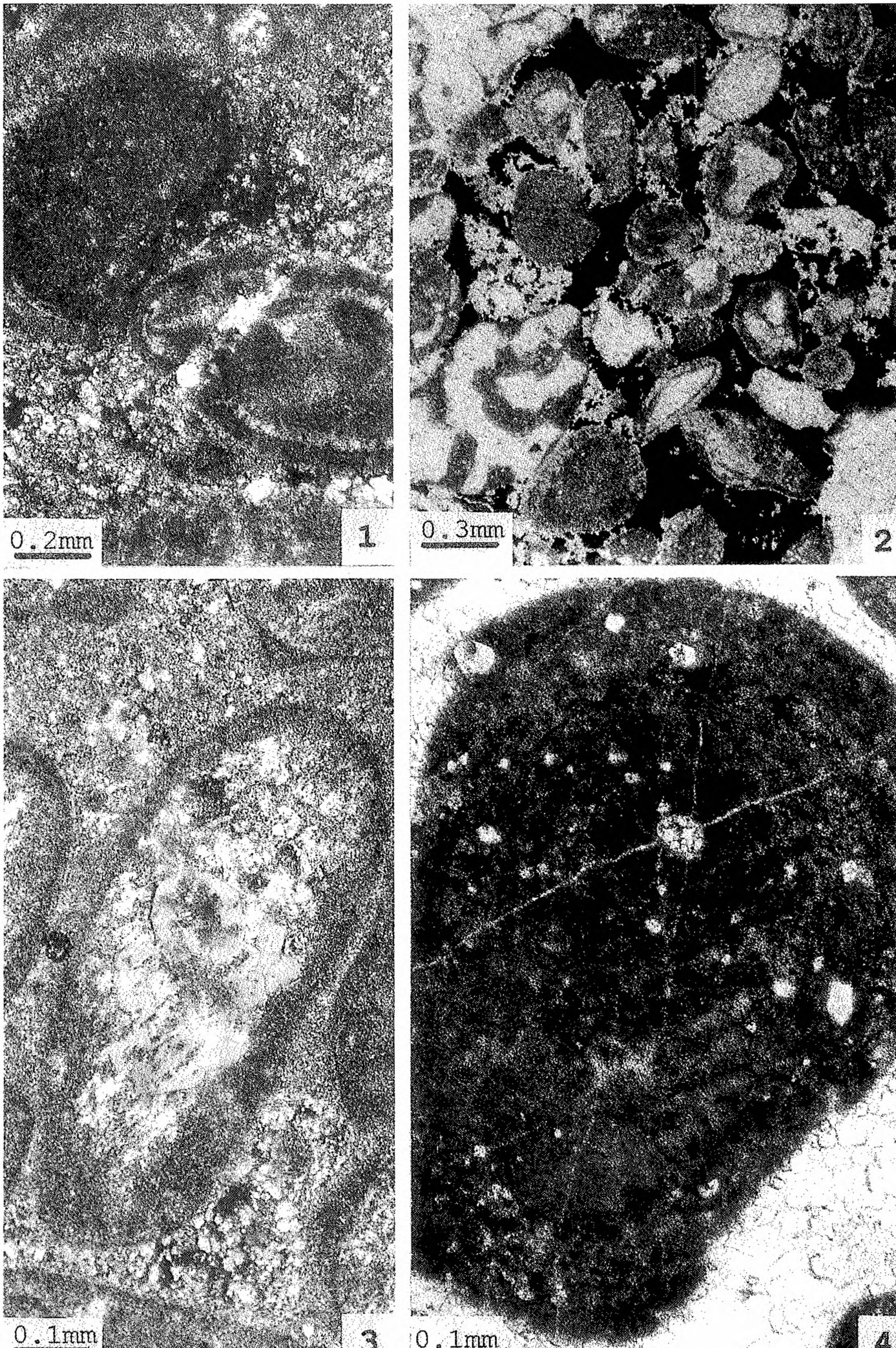
0.2mm
1
0.3mm
2
0.1mm
3
0.1mm
4

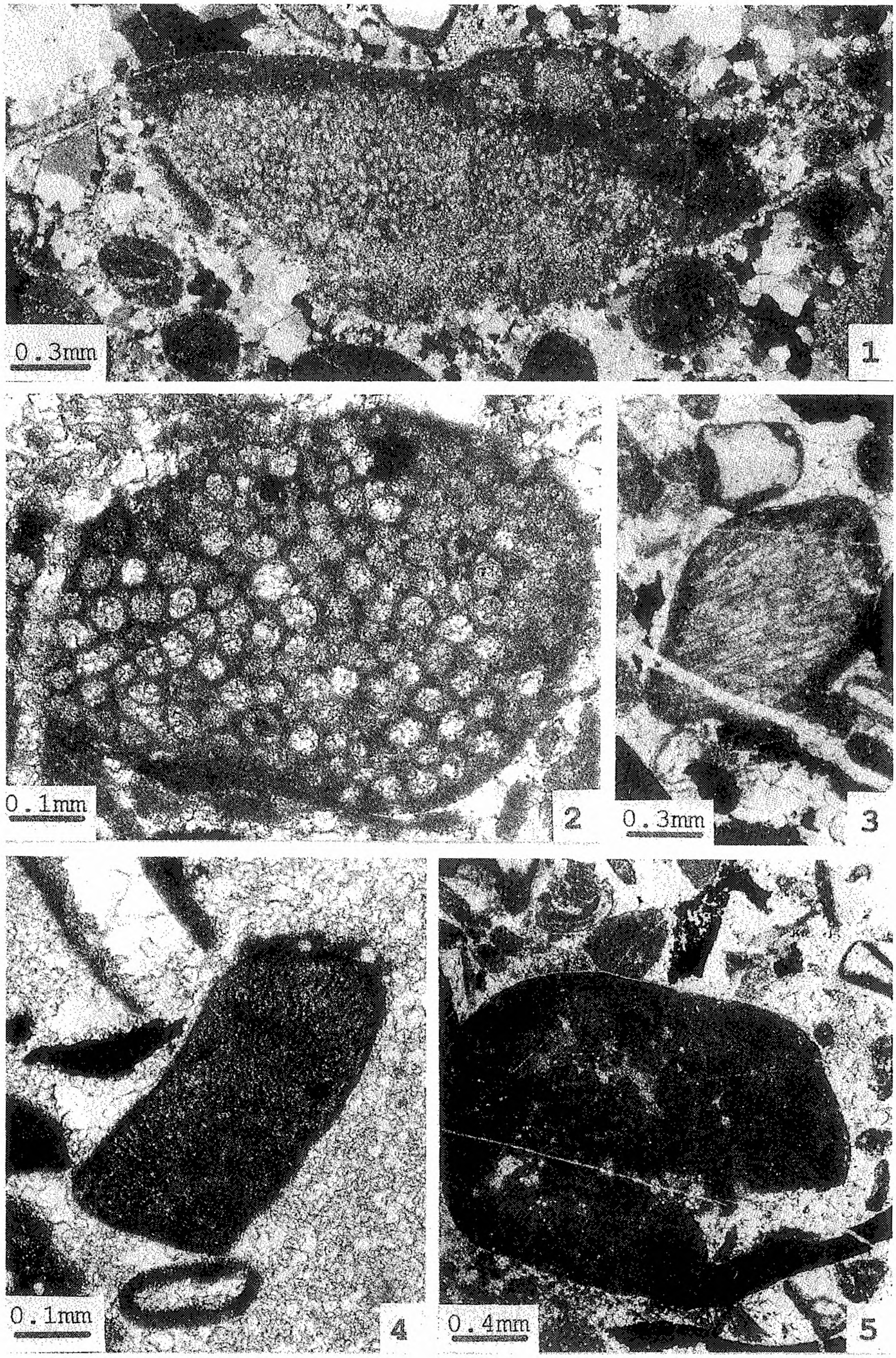
0.3mm
1
0.1mm
2
0.3mm
3
0.1mm
4
0.4mm
5

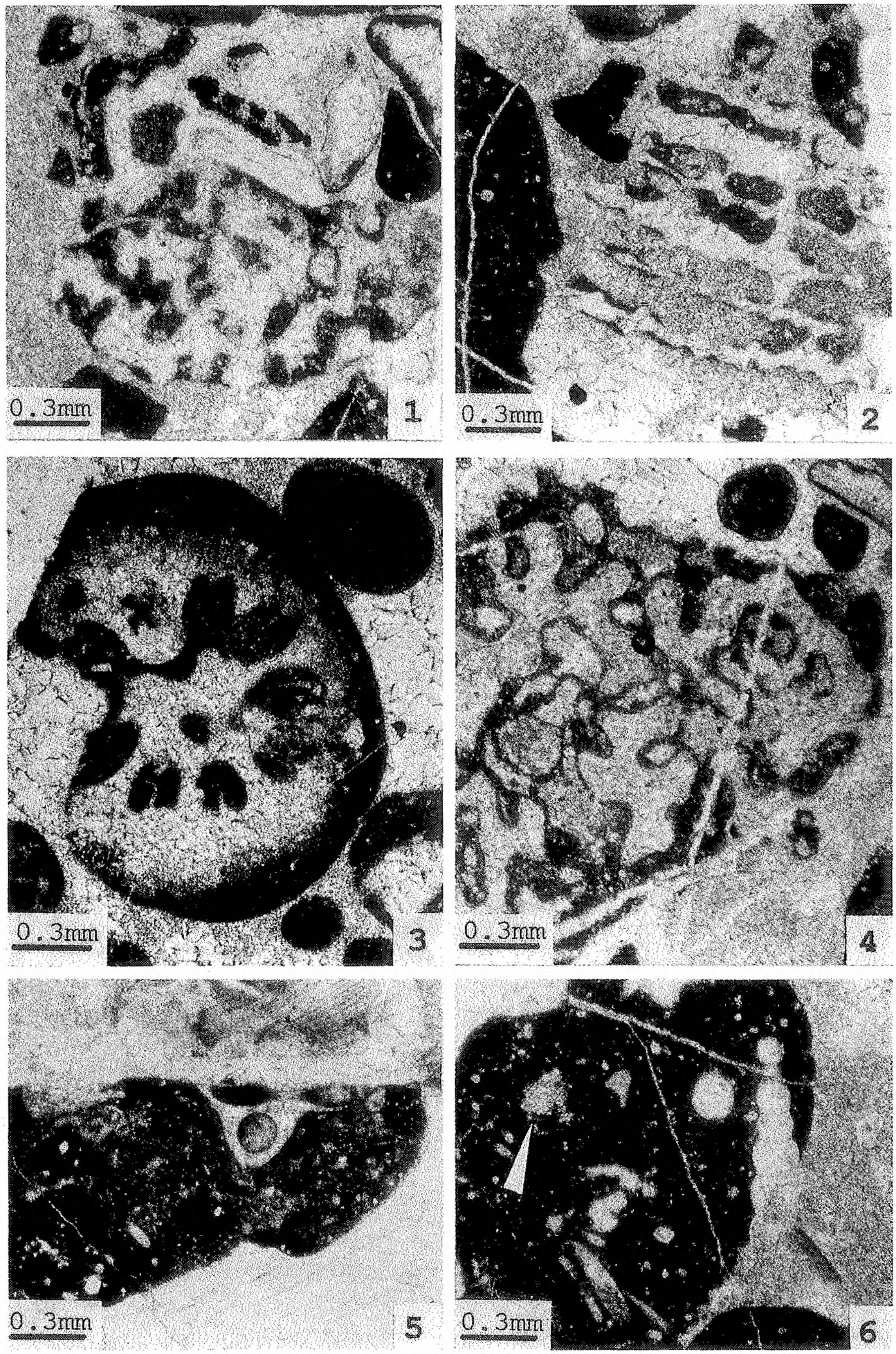
0.3mm
1
0.3mm
2
0.3mm
3
0.3mm
4
0.3mm
5
0.3mm
6

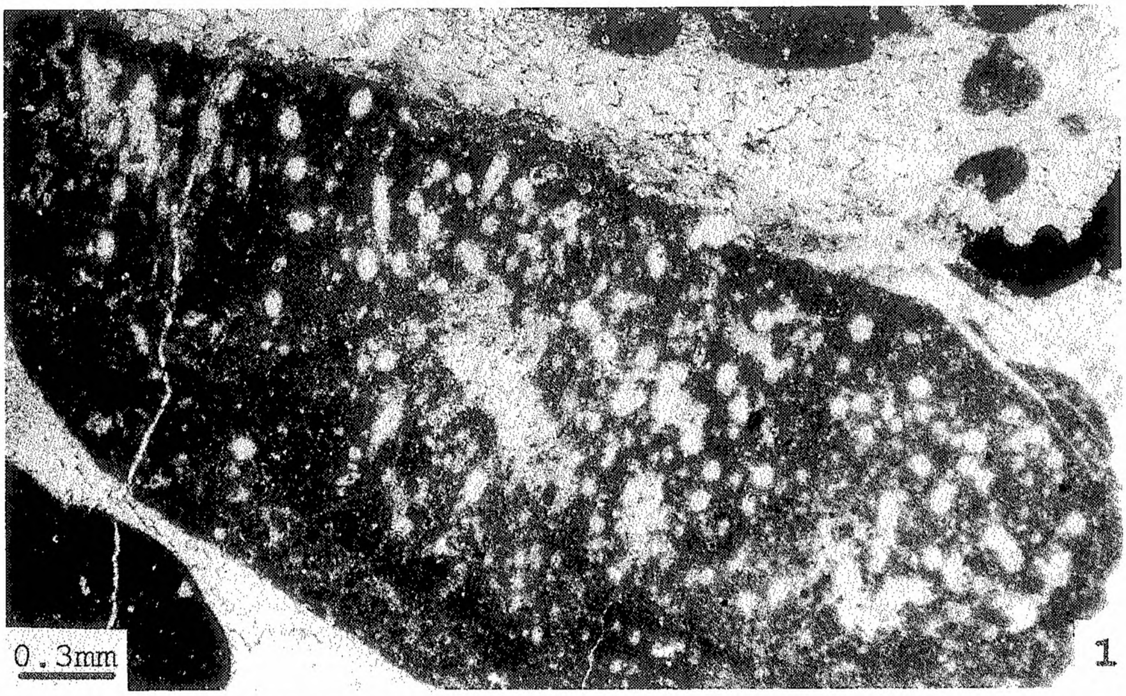
0.3mm
1


0.1mm
2

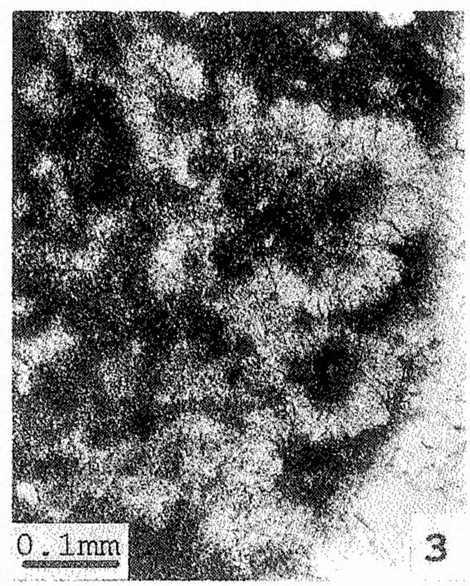
0.1mm
3

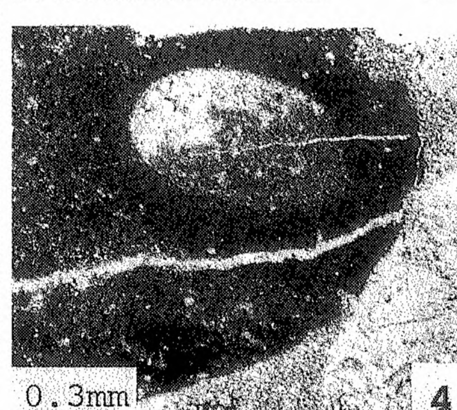
0.3mm
4

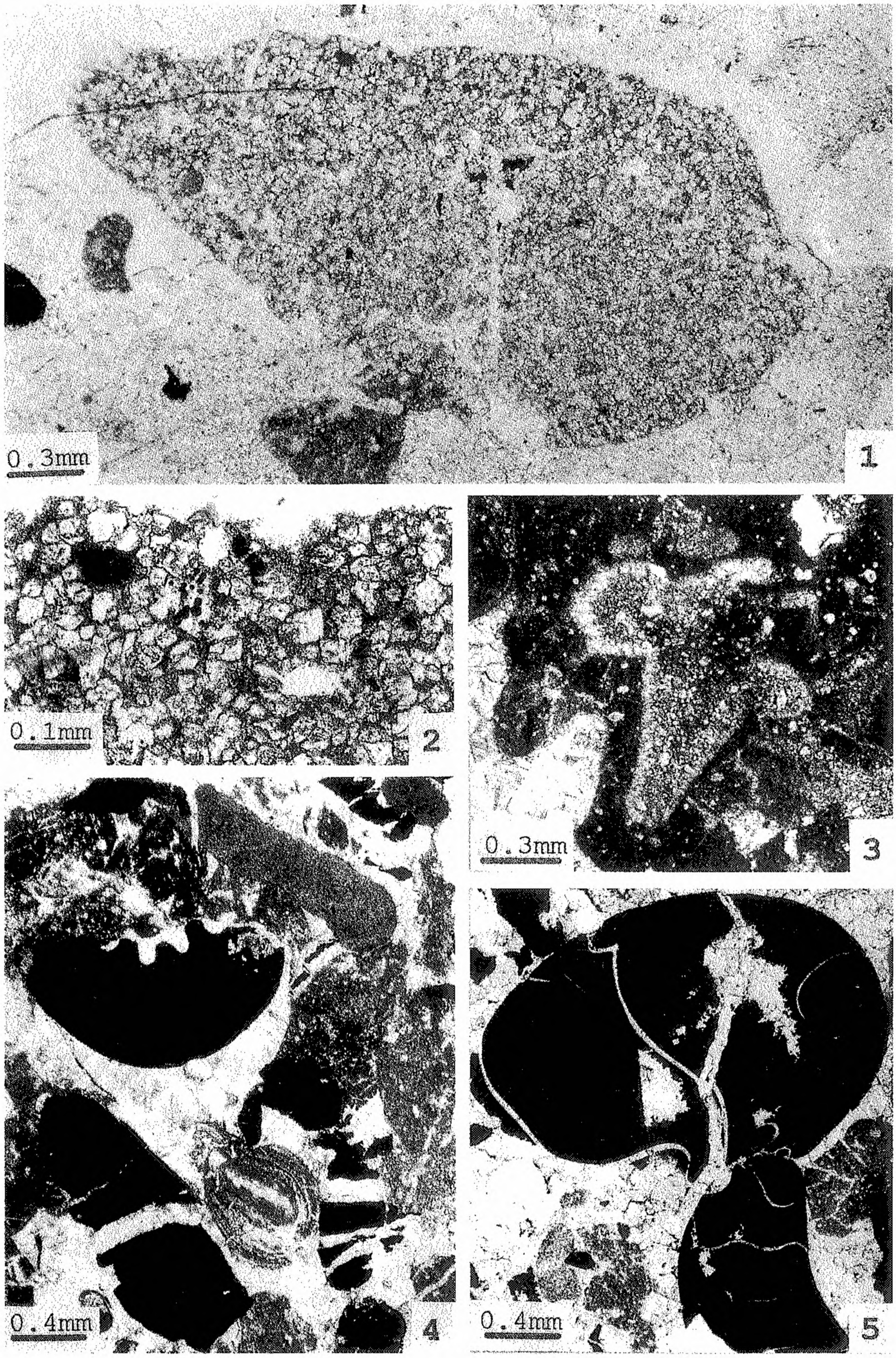
0.3mm
1
0.1mm
2
0.3mm
3
0.4mm
4
0.4mm
5

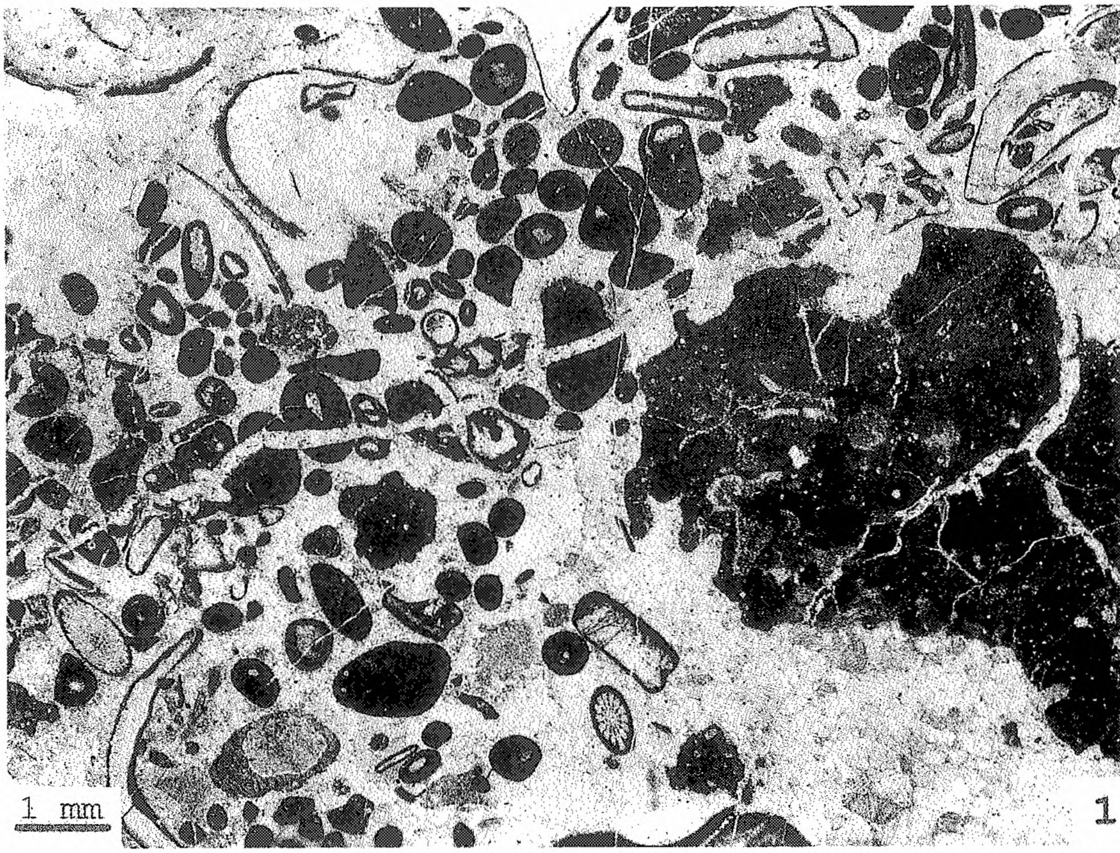
1 mm
1

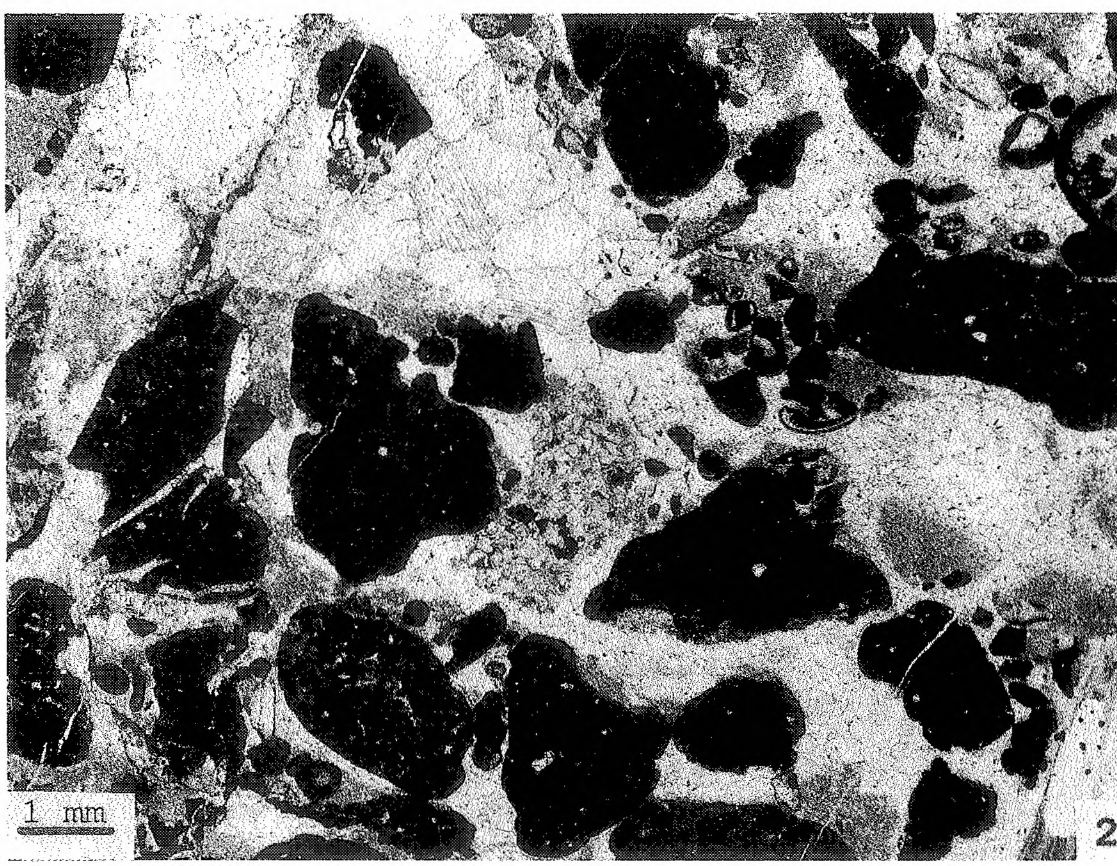
1 mm
2

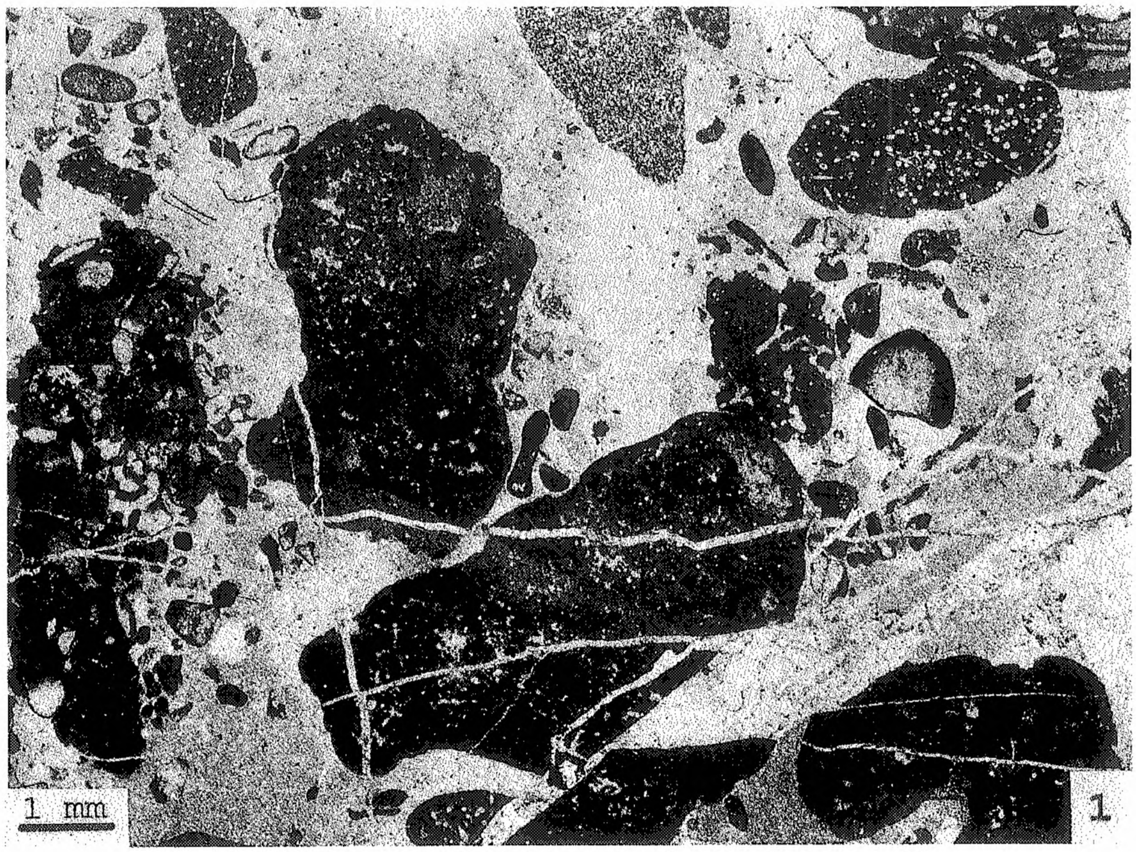
1 mm
1

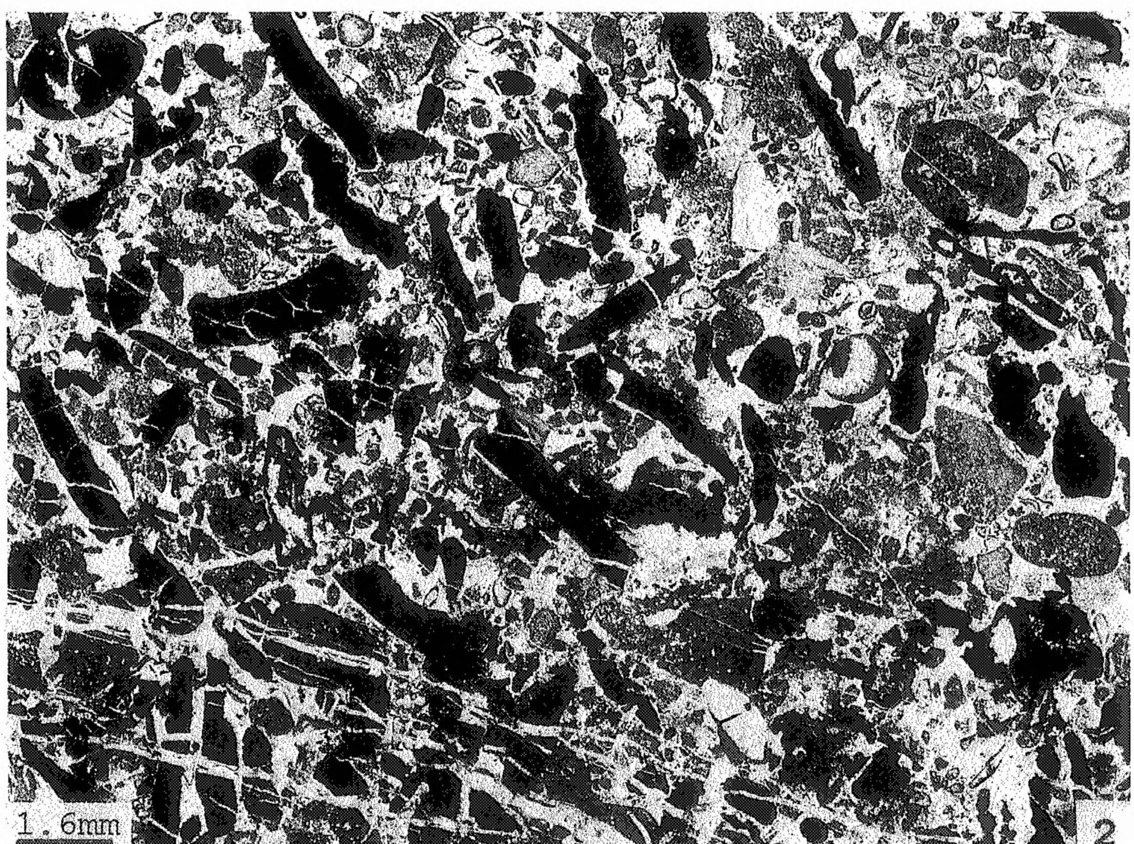
1.6mm
2

Przekrój poprzeczny przez koral. Facja gąbkowa.

4 — Hydrozoan fragment. Oolithic-sponge microfacies.

Fragment hydrozoa. Facja oolitowo-gąbkowa.

5 — Intraclast of cyanobacterial-spongeous limestone with transversal section of serpulae. Sponge microfacies.

Intraklast wapienia cyjanobakteryjno-gąbkowego. Widoczny przekrój poprzeczny przez serpulę. Facja gąbkowa.

6 — Intraclast with fragments of algae *Permocalculus* sp. (arrow) and partly dissolved gastropod shell. Vadose silt is visible right from the intraclast. Sponge microfacies.

Intraklast zawierający fragmenty glonu *Permocalculus* sp. (strzałka) i częściowo rozpuszczonego ślimaka. Na prawo od intraklastu wadyczny silt. Facja gąbkowa.

Plate (Plansza) VII

1 — Intraclast with quite well-preserved internal structure of calcitized siliceous sponge. Sponge microfacies.

Intraklast. Widoczna dość dobrze zachowana struktura budowy wewnętrznej skalcyfikowanej gąbki krzemionkowej. Facja gąbkowa.

2 — *Tubiphytes moronensis*. Central part of the oncoid is occupied by foraminifera *Nodophthalmidium* sp. and authigenic quartz crystal. Sponge microfacies.

Tubiphytes moronensis. Centralną część onkoidu zajmuje otwornica *Nodophthalmidium* sp. oraz kryształ kwarcu autigenicznego. Facja gąbkowa.

3 — Spherulites of inferred cyanobacterial origin. Sponge microfacies.

Sferolity o genezie prawdopodobnie cyjanobakteryjnej. Facja gąbkowa.

4 — *Terrebella lapilloides* Münster - polychaet typical of sponge facies. Arenaceous tube filled with geopetal infilling. Sponge microfacies.

Terrebella lapilloides Münster – wieloszczet typowy dla facji gąbkowej. Wewnątrz aglutynującej rurki widoczne wypełnienie geopetalne. Facja gąbkowa.

Plate (Plansza) VIII

1 — Dolomite intraclast with partial dedolomitization. Sponge microfacies.

Intraklast dolomitu wykazującego częściową dedolomityzację. Facja gąbkowa.

2 — Fragment of Pl. VIII: 1. Dark pigment filling intercrystalline spaces originates from iron oxides. Aggregates of minute spheroids are pyrite accumulations. Sponge microfacies.

Fragment Pl. VIII: 1. W obrębie intraklastu dolomitu widoczna ciemna substancja między kryształami pochodząca od tlenków Fe. Skupienia drobnych, ciemnych kulek są agregatami pirytu. Facja gąbkowa.

3 — Cavern in pelmicrite intraclast with walls covered with fibrous cement film and interior filled with dolomite crystals, partly dedolomitized. Oolithic-sponge microfacies.

Kawerna w intraklaście pelmikrytowym. Ścianki kawerny pokrywa powłoka cementu włóknistego, zaś wnętrze jest wypełnione częściowo zdedolomityzowanymi kryształami dolomitu. Facja oolitowo-gąbkowa.

4 — Pyritic-algal microfacies. Fragment of red algae *Marinella lugeoni* Pfender (upper right), pyritized bivalve shell (centre) and eccentric ooid (bottom).

Facja pirytowo-glonowa. Fragment krasnorostu *Marinella lugeoni* Pfender (u góry, z prawej), spirytyzowana muszla małża (w środku) i ekscentryczny ooid (u dołu).

5 — Pyritized shell of juvenile ammonite with well preserved suture lines. Pyritic-algal microfacies.

Spirytyzowana muszla juwenilnego amonita. Widoczne dobrze zachowane linie lobowe. Facja pirytowo-glonowa.

Plate (Plansza) IX

1 — Oolithic-sponge microfacies. Blocky sparry cement encloses numerous ooids, simple oncoids, fragments of bivalve shells and irregular intraclasts of cyanobacterial-sponge limestones with traces of dolomitization and dedolomitization.

Facja oolitowo-gąbkowa. W blokowym cemencie sparytowym występują liczne ooidy, onkoidy proste, fragmenty małżów i nieregularne intraklasty wapieni cyjanobakteryjno-gąbkowych ze śladami dolomityzacji i dedolomityzacji.

2 — Sponge microfacies. Numerous cyanobacterial-sponge limestone intraclasts show dissolution of the grain boundaries. Locally, vadose silt is present.

Facja gąbkowa. Liczne intraklasty wapieni cyjanobakteryjno-gąbkowych wykazują na krawędziach ślady rozpuszczania. Lokalnie nagromadzenia wadycznego siltu.

Plate (Plansza) X

1 — Sponge microfacies. Intraclasts of cyanobacterial-sponge limestones, dolomites (top) and pyritic matrix with abundant ooids. Locally, vadose silt is accumulated.

Facja gąbkowa. Prócz intraklastów wapieni cyjanobakteryjno-gąbkowych obserwuje się także intraklasty dolomitu (u góry) i intraklasty zawierające liczne ooidy w pirytowym matriks. Miejscami nagromadzenia wadycznego siltu.

2 — Pyritic-algal microfacies. Two main components are visible - dark, angular grains of detrital pyrite and numerous, rounded algae fragments.

Facja pirytowo-glonowa. Widoczne dwa podstawowe składniki: ciemne, ostrokrawędziste ziarna detrytycznego pirytu i liczne, oble fragmenty glonów.